UNDERSTANDING THE SOURCES OF VARIABILITY DURING IN VIVO RAMAN SPECTROSCOPY MEASUREMENT OF HEALTHY HUMAN SKIN

By

Isaac James Pence

Thesis

Submitted to the Faculty of the

Graduate School of Vanderbilt University

in partial fulfillments of the requirements

of the degree of

MASTER OF SCIENCE

in

Biomedical Engineering

August, 2012

Nashville, Tennessee

Approved:

Professor Anita Mahadevan-Jansen

Professor Darrel L. Ellis

ACKNOWLEDGMENTS

I would like to acknowledge the financial support that enabled the completion of this project, especially the numerous National Institutes of Health grants, which funded the Raman equipment used during this study.

I would like to thank my advisor, Dr. Anita Mahadevan-Jansen, for her guidance through all of my research endeavors, and for her constant trust and support. Thank you for taking the chance on me and continuing to help me develop as a researcher.

This work would not have been possible without the guidance and collaboration of many members of the Biomedical Photonics Laboratory. Special thanks to Dr. Elizabeth Vargis and Dr. Chetan Patil for teaching me so much about the instrumentation, procedures, analysis, and every other skill used to conduct this research. Christine O'Brien and Dr. Quyen Nguyen were also instrumental throughout the development of the work for the assistance, feedback, and guidance they provided.

I would also like to thank my parents, family, and friends for their humor and support when nothing ever goes as planned.

TABLE OF CONTENTS

LIST OF TABLES

Table Page

LIST OF FIGURES

Figure Page

CHAPTER I

INTRODUCTION

Overview of Skin Cancer

Skin cancer is the most prevalent cancer in the United States, and in 2012 is estimated to be diagnosed in over 2 million new cases, resulting in roughly 12,000 deaths.[1] Because the classification and prognosis of skin cancer depends on the cells from which the cancer originates, two primary sub-groups have been delineated: melanoma and non-melanoma skin cancers. Accounting for fewer than 5% of skin cancer cases, melanoma skin cancers are responsible for a majority of related deaths. An estimated 70,000+ melanoma cases will be diagnosed in the US during 2012 with incidence varying based on age, gender, and skin type. Alternatively, non-melanoma skin cancers are primarily accounted for by basal cell carcinoma (BCC) and squamous cell carcinoma (SCC). Originating in the deepest layer of the epidermis, roughly 80% of skin cancers are BCC, while the more aggressive SCC type account for most of the remaining 20%. Both of these cancers commonly appear on sun-exposed areas of the body like the face, ears, neck, back, and hands.[2, 3] The risk of developing skin cancer is associated with Ultraviolet (UV) light exposure, presence of moles, fair skin, old age, previous skin cancer diagnosis, suppressed immunity, and smoking. Diagnosis of these malignancies is usually performed by visual inspection followed by biopsy to improve specificity, although other tools are becoming available. Accurate staging of the disease progression allows doctors to provide optimal treatment options to attain positive outcomes and

improve quality of life. Typical treatment options include surgery, local and systemic chemotherapy, immunotherapy and radiation therapy but the proper choice is both case and skin cancer-type dependent.

Normal Skin: Form and Function

As the largest organ in the body, the skin is composed of an array of components and specialized cell types and is the fundamental barrier between the body and the environment. The skin plays a vital role in sensory reception, thermal regulation, immunological surveillance, fat and water storage, and protection against light, injury, and infection. To distinguish between both the structures and functions, the skin is divided into three main sublayers: the epidermis, dermis, and subcutis, which are depicted in Figure I.1. The skin is further divided into two descriptive groups based on inherent structures. The glabrous (non-hairy) skin, found on the palms of the hands and soles of the feet, has a uniquely patterned, grooved surface of alternating ridges that constitute a person's dermatoglyphics (ie, fingerprints). This skin is characterized by a thick epidermis divided into well-defined layers and contains encapsulated sense organs in the dermis but no hair follicles or sebaceous glands. Hair-bearing (non-glabrous) skin has both hair follicles and sebaceous glands, but encapsulated sense organs are absent. Because of this change in composition, the hair acts as the sensory structure. Non-glabrous skin composition is also highly variable between unique body sites.[4]

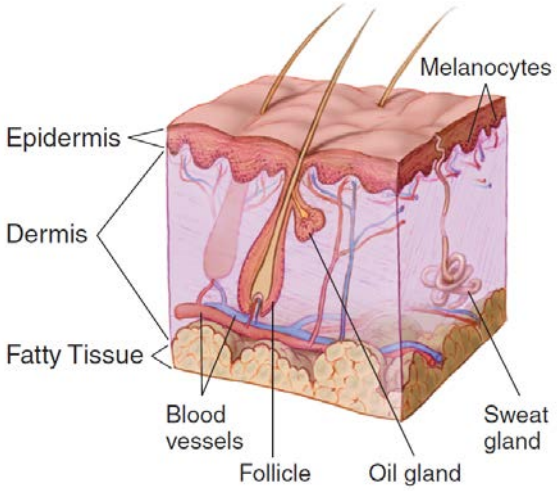

Figure I.1. Diagram of macroscopic view of skin.[5]

The epidermis is the outermost layer of skin tissue and has a layered composition. This avascular superficial layer is composed largely of keratinocytes, approximately 95% of the total cellular composition, that are formed by proliferation of the deeper layer of basal cells. Other native cell populations occur with differing frequency depending upon the level of the epidermis. At locations where hair follicles are present, the superficial epidermis extends deep into the skin forming a continuous pocket. This structure has a small segment of smooth muscle connected from the dermis to the follicle wall. Above the point of insertion, the sebaceous, or oil-producing, glands open into the follicle canal. The eccrine sweat glands of the epidermis open directly to the skin surface and are present in every region of the body.[4]

The epidermis is further divided into multiple layers. The outermost surface, the *stratum corneum*, is composed of large, flattened, dead polyhedral cells, or squamous cells, that are continuously shed as newer ones are formed. These cells have lost nuclei and cytoplasmic organelles, and the connective keratin filaments have aggregated into

cross-linked macrofibers. The more superficial the squamous cell, the more exaggerated the flattening. Only for the palmoplantar skin, a layer beneath the *stratum corneum,* called the *stratum lucidum*, is formed by three to five layers of dead flattened keratinocytes. The thickness and coloration of this region is controlled by the rate of mitosis of the epidermal cells and the presence of melanocytes in the tissue, respectively. The cells here are still nucleated and are often referred to as "transitional cells." The next layer, the *stratum granulosum* is where the most highly differentiated viable keratinocytes of the epidermis are located. These squamous cells are called granule cells due to keratohyalin content, a protein that forms dense cytoplasmic granules that promote cell dehydration and keratin aggregation and cross-linking. The cellular cytoplasm also contain lamellated granules that discharge lipid content into the intracellular spaces affecting barrier function and intercellular cohesion.[4] Descending further, the *stratum spinosum* comprises the first suprabasal layer of cells where adjacent cells are joined by adhesive desmosomes. The cells at this level are enlarged keratinocytes and contain typical cellular organelles, microfilaments, and melanosome-complexes, beginning as polyhedral-shaped cells that flatten during ascent to the skin surface. The deepest layer of cells associated with the epidermis is the *stratum germinativum,* a continuous layer of basal cells. These pluripotent cells are small, cuboidal cells with large nuclei, dense cytoplasm, and numerous ribosomes. They remain undifferentiated and reproduce regularly to maintain skin cell turnover.

Other structures that are of vital importance to the skin are melanocytes, Merkel cells and Langerhans cells. Melanocytes are the pigment-synthesizing cells and are generally confined to the basal layer with projections extending into the spinous layer

toward the skin surface. Keratinocytes are thought to phagocytize the processes of these uniformly distributed melanin producing cells and incorporate the melanin storing organelles, melanosomes, into caps within the cytoplasm positioned above the keratinocyte nucleus. This integration of melanosomes effectively distributes the skin pigment in a more homogeneous manner and affords better protection from incident light.[6]

A major nerve cell type located in the epidermis is the Merkel cell. These cells connect to an enlarged nerve terminal as a mechanical receptor for discrimination of light, sustained touch sensations. Merkel cells have a lobulated nucleus, characteristic granules in the cytoplasm, underlying nerve plate, and are associated with slow-adapting somatosensory nerve fibers. These have been found in all vertebrates, and are especially common in the *stratum germinativum.* An often missed and dangerous cancer type, the Merkel cell tumor, derives from this cell type. Merkel cell tumors have one of the lowest survival rates and diagnosis is often missed due to clinical appearance.

Another cellular population of the epidermis is the Langerhans cells. These cells are derived from precursor cells originating in the bone marrow and continually repopulate the epidermis.[6] Similar to melanocytes, the Langerhans cells have a lobulated nucleus, pale cytoplasm, and extended dendritic processes among keratinocytes. The cell types are differentiated by the presence of Langerhans cell granules, which are disc-like vesicles. The function of these granules is still unknown, but they have been identified in many other species and cell types. The role of the Langerhans cells has also been debated, but is thought to participate in antigen processing for the skin's immune system.

Responsible for the separation of the epidermis from the dermis, the basement membrane, or dermal-epidermal junction, is a complex structure involving cells and extra-cellular matrix of both contiguous regions. This multi-layered barrier is connected by microfibrils and hemidesmosomes linking the layer of basal cells to the basal lamina and in turn to the reticular lamina. This network of anchoring fibrils continues deeper into the dermis, where it either terminates in a bush-like formation or loops back into the basement membrane and basal cell layer.[6] Along with its role of mechanical support, this barrier serves as a size- and charge-selective filter, inhibiting anionic macromolecules and cells from deeper passage.

The dermis is the lower section of the skin located beneath the basement membrane. It is composed primarily of a supporting, extrafibrillar matrix or ground substance in which polysaccharides and proteins are interlinked to produce water storing macromolecules and impart bulk, density, and strength to the skin. Also present are high tensile strength collagen fiber bundles, the primary dermal constituent, and elastin fibers, the assembly, size, and density of which help to separate the region into layers involved in protection from disease and environmental attack. An array of fibroblasts, mast cells, and histiocytes comprise most of the remaining cells in the dermis.[4]

The superficial dermal layer is the papillary dermis and contains bundles of small-diameter collagen fibrils. Including the invaginations in the region of the basement membrane, elastin fibers are present only in cross-linking or as a soluble coating around microfibril bundles. Cells are more abundant in the papillary dermis, fibroblasts have greater mitotic activity and there is a high density of blood vessels. At the deepest part of this layer is a horizontal plexus of blood vessels, forming a border with the deeper,

reticular dermis. From here, capillary loops extend superficially toward the epidermis to aid in thermoregulation and provide nutrients via diffusion.

The papillary dermis contains multiple sensory receptor types. Meissner's corpuscles are fast-adapting sensory receptors for light, fluttering touch. Found deeper within the dermis are the Ruffini endings, which respond to deep, sustained mechanical pressure and stretch of the skin. The deepest layer of the dermis, the reticular dermis, is the outermost perfused layer of the skin. This region accounts for the bulk of the dermis, and includes large bundles of collagen fibrils and mature elastic fibers with a high proportion of elastin relative to the microfibrillar components.[6] These elastic fibers are generally found between the collagen bundles.

Despite the lower cellular density of the reticular dermis, fibroblasts, mast cells, and macrophages are found in the interstitium between collagen bundles. The fibroblasts of the dermis are responsible for the synthesis, destruction, and remodeling of connective tissues. The shape of these cells is site-specific, but they are commonly located between bundles of collagen or in close association with individual collagen fibrils or elastic fibers. Nerve endings, the pacinian corpuscles, which are rapidly-adapting sensors of vibrations and deep pressure, are also present in the dermis. The macrophages found in the dermis range from early-development to fully-differentiated stages depending upon cellular surface markers. The late-stage macrophages are large with at least one nucleus and an abundance of lysosomes and phagocytic vacuoles. These cells are involved in the synthesis and secretion of hydrolytic enzymes, soluble factors affecting T-lymphocyte activity, prostaglandins, and interferon. Mast cells are specialized secretory cells that are common in the connective tissue matrix. Most common in the upper dermis, around

vessels, and around subcutaneous fat, Mast cells accumulate around sites of inflammation and wound repair.

Beneath the dermis is a layer known as the subcutis (hypodermis or subcutaneous layer). Together with cells in the dermis, the subcutis forms a network of collagen and fat cells. This layer also helps to conserve body heat and acts as a shock-absorbing layer to protect internal organs. The contents of the subcutis are highly varied, including loosely arranged elastin fibers, fibrous bands anchoring the skin to deep fascia, fat, blood vessels destined for the dermis, lymphatic vessels from the dermis, hair follicle roots, the free endings of nerves and Pacinian corpuscles, bursae overlaying the joints to facilitate movement, and fine, flat sheets of muscle. The subcutis is composed primarily of adipocytes, cells specialized for the accumulation and storage of fat. These adipocytes are grouped into lobules and separated by connective tissue.

Aging of Skin

The aging process of skin has been clearly observed for many years primarily due to the ease of access to the tissue. Despite the highly individualized variability, the process is characterized by the overall physiological decline with increasing age. More recently, distinction has been made between inherent aging changes and age-related environmental changes, developmental changes, and age-related diseases. The most common and most important of these aging processes is “premature aging” induced by chronic sun exposure. This photo-aging is responsible for most of the clinically evident age-associated cutaneous change.

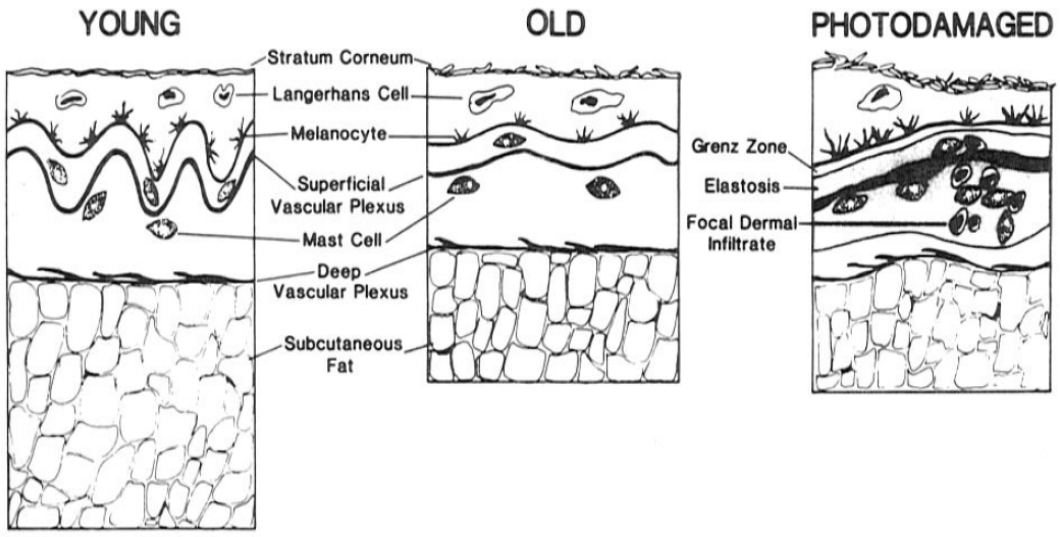

Figure I.2. Histological features of young, old, and photodamaged skin.[6]

Morphologically, the majority of aging change in sun-protected skin includes increased roughness, fine-wrinkling, laxity, and proliferative lesions. In sun-exposed skin, along with the aforementioned changes, the skin can experience elastosis (a pebbly, yellowed quality due to changes of elastic fibers), irregular hyperpigmentation and depigmentation, coarse wrinkling, and actinic keratosis. Histologically, the most striking change with aged human skin is the flattening of the dermal-epidermal junctions, as seen in Figure I.2, which causes a reduced transfer of nutrients, a smaller surface between the neighboring compartments, and a reduced resistance to shearing forces. For protected skin, the variability in epidermal thickness and keratinocytic size increases with age. The dermal microfibril bundles anchoring the basement membrane are reduced. Decreases in the number of enzymatically active melanocytes per unit surface area of the skin have been documented, reducing the body's protection against UV light.[6] Langerhans cells are thought to be reduced by 20 to 50% between early and late adulthood and may account for the decreased immunological response of aged skin. Dermal thickness has been

reported to decrease gradually with age, and a significant age-related loss of the dermal vascular bed and vertical capillary loops are believed to underlie many of the physiologically atrophic changes of aged skin. Loss of elastin fibers may result in the appearance of fine wrinkles and elastosis is believed to contribute to more pronounced wrinkling in photo-aged skin. Deep wrinkles associated with expression lines are thought to be caused by contractions of connective tissue within the subcutaneous fat.[6]

Changes in the color, density, and distribution of hair are widely recognized results of skin aging. Graying is caused by a progressive depletion of melanocytes from the hair bulb. Gray hairs may have remaining melanocytes with vacuoles, while the hair shafts contain fewer melanin granules than the normally pigmented hairs. The loss of melanocytes is thought to occur more quickly within the hair than the skin. The decreasing frequency of Meissner's and Pacinian corpuscles, and increasing variation in size and distribution, of the nerve endings responsible for detection of light touch, lead to a decreased perception of low pressure mechanical stimuli.

Age-related decreases in the turnover of epidermal cells have been documented due to rates of desqumation, or shedding, of the *stratum corneum*. The replacement rate of surface cells decreases with age and causes the tissue to exhibit fewer of the traits of young, healthy skin. Many of the inter-related functions of the human skin that are affected with age can be found in Table I.1. The repair rate declines with age, especially in relation to wound closure, epidermal cell migration and mitosis, collagen deposition, and development of wound tensile strength.[6] Because of the constant replication of cells in the basal layer of the epidermis, neoplasia is especially characteristic of aging skin. The prevalence of these growths is almost ubiquitous as explained by Soter. "One or

more benign proliferative growths are present in nearly every adult beyond the age of 65 years, and most adults have dozens of lesions." [6] A decrease in chemical clearing and the barrier function of the *stratum corneum* is reported for several substances as well as a decrease in sensory perception in old skin. The decreased immune function of the skin is presumed to impact the increased propensity for disorders such as skin cancer with increased age.

Table I.1. Functions of Human Skin that decline with age Adapted from ref (6).

Cell replacement	Immune recognition
Injury response	Vascular responsiveness
Barrier function	Thermoregulation
Chemical clearance	Sweat production
Sensory perception	Sebum production
Vitamin D production	Mechanical protection

Structure of Common Skin Lesions

As the exterior surface of the body, the skin affords opportunities for clinical and pathologic correlation due to its ease of access for physical examination and visual inspection. Due to the variety of potential lesions which denote significant and unique changes within the skin, it is important to have a working understanding of the common lesions associated with malignant and benign pathologies of melanoma and non-melanoma lesions. A macule is a flat, distinct, colored area of skin that does not include a change in skin texture or thickness. It may result in any layer of the skin and any size or shape. The distinctive variation in color can result from epidermal hyperpigmentation (Figure I.3, i-A), dermal pigmentation (i-B), vascular dilation (i-C), or extravasated

erythrocytes (i-D). A papule is a small, solid, rounded bump rising from the skin that is usually less than 1 cm in diameter. The majority of these lesions are found above the plane of the skin and can result from metabolic deposits (Figure I.3, ii-A), cellular infiltrates in the dermis (ii-B), or localized hyperplasia of cellular elements in the epidermis or dermis (ii-C). Papules may open when scratched and become crusty and infected. The variation in color and shape of these lesions can be used clinically to differentiate several lesion types. Plaques are elevated, solid, superficial lesions more than 0.5 cm in diameter. A plaque tends to be flat over the whole surface and is often formed by confluent papules. A nodule is a palpable, solid, round or ellipsoidal lesion of varying size in either the dermis (Figure I.3, iv-A) of the epidermis (iv-B). A large nodule is a tumor, a term that can also apply to any mass, benign or malignant. A corresponding description of the nodule surface is also vital to differentiating lesion types. Drawings of each of these lesion structures can be seen in Figure I.3, to better understand the given explanation.

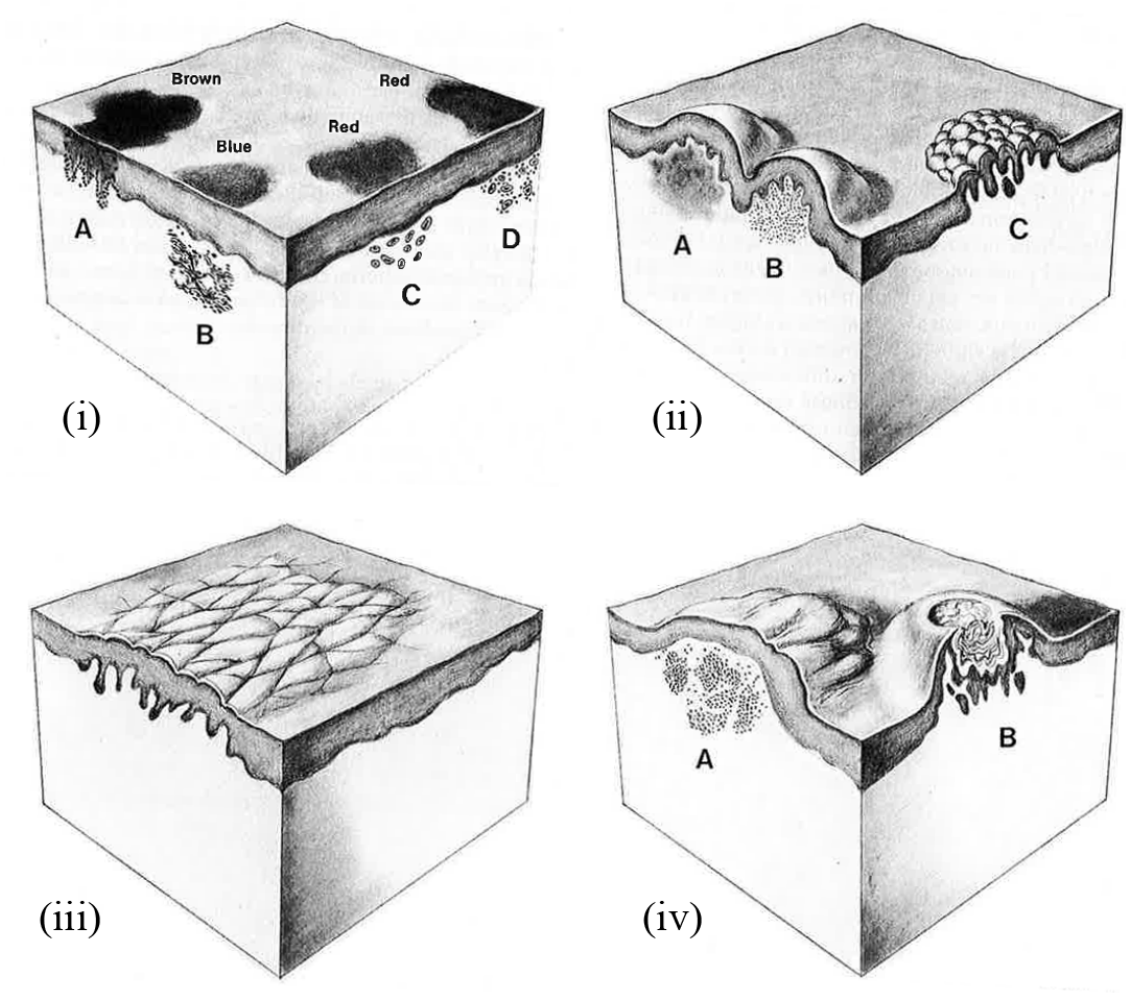

Figure I.3 (i-iv). Macroscopic structure of skin lesions for macule (i), papule (ii), plaque (iii), and nodule (iv). Letters correspond to specific structures mentioned in the text.[6]

Risk Factors for Skin Cancer

There are many risk factors associated with the development of skin cancers, some having higher associated risks than others. The most indicative of these factors is exposure to UV radiation. This band of light has the potential to damage genes and alter cellular reproduction. People with higher accumulated lifetime exposure levels to these wavelengths of light are at an elevated risk. This light can come from natural sunlight, sunlamps or tanning beds. Fair skinned people, usually with blond or red hair and light-

colored eyes, are at an increased risk, but people that have darker complexions or different skin types are also susceptible. The amount of UV radiation exposure is highly dependent upon the person's lifestyle and geographic location, with increased exposures for latitudes nearer to the equator or high elevations. The UV band of the radiation spectrum can be divided into three categories: UVA, UVB, and UVC ranges. The UVA grouping, or long wave UV, has wavelengths that range from 315 to 400nm. These wavelengths can cause some damage to cellular DNA, reduce the cancer surveillance for skin immunity, and are primarily linked to long-term skin damage like wrinkles. The midrange UVB rays, from 280 to 315nm are considered to be the primary cause of skin cancer, as these rays can cause direct damage to cellular DNA, and are responsible for most sunburn cases. The UVC grouping, from 100 to 280nm, do not penetrate the Earth's atmosphere and therefore are not considered a common cause of skin cancer. A subset of the population, including pilots and astronauts, are monitored for increased exposure to these UVC rays and are at an increased risk of developing skin cancer. These UV wavelengths are a primary cause of skin cancer due to the damage that they inflict on the DNA and genes that control cell growth. The subsequent uninhibited proliferation of cells can lead to the development of cancerous lesions. The amount of UV exposure depends not only on the intensity of the radiation but also on the duration of exposure and the level of protection afforded to the skin by clothing, sunscreen, or other layers. A noted misconception that having a sun-tan will protect even a fair-skinned person from skin cancer must be discredited.[7]

Frequent sunburns during childhood and high levels of exposure at a young age are also added risk factors. Fair skin is considered a factor increasing the risk of skin

cancer, as the protective melanin of less pigmented, fair skinned people is lower than in those with darker skin.[3] The presence of scars, burns, or other long-term inflammatory conditions also predisposes people to the development of skin cancer. Increased exposure to certain chemicals, including arsenic, causes an increased risk. HPV infection and reduced immunity have been linked to increased risk of developing skin cancer. The presence of actinic keratosis or Bowen's disease can develop into squamous cell carcinomas.[3] Development of malignant melanoma occurs in up to 5% of total melanoma cases in people with congenital nevi and those who develop dysplastic nevi have an approximately 50% cumulative lifetime risk for melanoma.[8, 9] While recurrence is strongly linked to lesion depth, the likelihood of developing a subsequent melanoma is also significantly increased compared to the rates of initial lesion development, and rates increase with positive family history for the pathology.[5] Several other risks associated with malignant melanoma are listed in Table I.2.

Table I.2. Risk factors for malignant melanoma (MM). Adapted from ref (10).

Specific MM Risk Factors	**Relative Risk**
Melanocytic Nevi (MN)	
Atypical Mole Syndrome	
No personal or family history of MM	2-92
Personal but no family history of MM	8-127
(II) 1 family member with MM	33-444
(III) ≥2 family members with MM	85-1269
>50 common MN	2-64
Congenital MN	17-21
Phenotypic traits	
Freckles	3-20
Fair complexion	2-18
Blond hair	2-10
Red hair	2-6
Tendency to sunburn	l-5
Inability to tan	2-5
Blue eyes	2-3
Sun exposure	
Constant	2-5
Intermittent	2-3
Immunosuppression	2-8
History of non-MM skin cancer	3-17

Skin Cancer types

Skin cells, like most cells in the body, reproduce rapidly early in life to allow the body to grow and develop. As a person reaches adulthood and proliferative rates decrease, skin cells normally grow and divide to form new cells needed only to maintain proper function. As the cells age and decrease in functionality, they die and are replaced by newer cells. Occasionally this process is altered and the body produces unneeded, new abnormal cells or old cells do not die off. Such cells accumulate to form a tumor which can be benign, pre-malignant, or malignant. Benign tumors are in general, rarely life threatening, can be removed with little chance of recurrence, and seldom do constituent cells spread to neighboring tissues. For cancerous or malignant growths, removal can often occur, but regrowth is possible. These malignant growths are more serious and may be life threatening. The cells of these growths can invade and damage nearby tissues and organs or enter the blood stream or lymphatic organs through a process known as metastasis. Depending on the type and location of the primary cancer (site of the original tumor), the spread of cancer can have a wide range of metastatic targets.

As mentioned above, the cancers that form in human skin are divided into two major subgroups: cancers originating in melanocytes and those that do not. This second, broad and somewhat vague classification is mainly composed of cancers called keratinocytic carcinomas as the cells share common features with the keratinocytes of the epidermis. Both of these malignant subgroups have associated benign lesions that must be well characterized for proper discrimination between the serious cases of cancer and the less worrisome benign or pre-malignant growths. First the cases of non-melanoma type cancers will be handled. Within this subsection, basal and squamous cell carcinomas

are the most common forms of skin cancer, generally appearing on the head, face, neck, hands and arms.

Non-melanocytic Skin Cancer

Basal cell carcinoma (BCC) is so named because it is thought to originate from freely differentiating cells in the basal layer of the epidermis. The cells present in these tumors also have many features in common with the cells of the exterior skin layer. Accounting for almost 80% skin cancers and as the most common malignancy in white people, these cancers are thought to result primarily from increased levels of exposure to the damaging rays of the sun.[3] These lesions tend to grow slowly, are generally asymptomatic aside from crusting, and rarely spread to nearby lymph tissue or distant sites in the body. If left untreated, these lesions can grow deep in the tissue, through the basement membrane and even into deeper structures like bones. The incidence of this cancer shows high geographical variation, and in North America, there is a 30% lifetime risk of acquiring this malignancy.

While increased exposure to UV radiation is a major causative factor, this alone does not seem sufficient to account for the wide variation in appearances of the lesions, nor for the occurrence in some people and not others.[11] Personal susceptibility depends greatly on interactions between intensity and duration of exposure to UV radiation and genetic makeup. Lesions that are present in clusters or develop on the trunk, are each associated with distinct predispositions. Those with basal cell carcinomas of the trunk generally have more total BCC lesions, are younger, and develop more clusters.[11] The appearance of these lesions also varies markedly depending upon location on the body.

Roughly 80% of these lesions appear on the head or neck. Early BCCs are commonly small, translucent or pearly, with raised areas through which dilated vessels may show. The classic presentation is a hardened edge and ulcerative center. Other patterns include nodular or cystic, superficial, morphea form and pigmented. Superficial BCCs generally occur on the trunk, are often flat and particularly slow growing, potentially mimicking psoriasis, eczema or Bowen's disease. The most important clinical subtype, accounting for 5% of BCCs, is the morphea form BCC due to its aggressive nature, late presentation, and difficulty in both diagnosis and complete excision. Patients with this lesion have an increased likelihood to develop another BCC or an SCC and the lesions can commonly be misdiagnosed as scars, SCCs, malignant melanomas, melanocytic nevi, or Bowen's disease among others.

Squamous cell carcinoma (SCC) accounts for two in every ten cases of skin cancer and commonly appears on sun-exposed (actinically damaged) areas of the body. These erythematous lesions have varying degrees of scaling and crusting.[6] These lesions develop on sun-protected areas as well as scars or skin ulcers, sometimes beginning as actinic keratosis (described below). The lesions that form on sun-exposed areas are most commonly found on body parts that receive the highest levels of irradiation including the top of the nose, the forehead, and the lower lip. This subgroup of SCCs is similar in behavior to BCCs, with the exception of lip SCCs, which are more aggressive. When SCCs occur in sun protected regions, the lesions tend to be more aggressive, more likely to invade nearby fatty and lymph tissues or metastasize. The SCCs commonly occur as multi-nodular tumors with surface loss due to abnormal epidermal cells or poorly defined nodules or plaques with crusting or eroded surfaces. Often these tumors are red and

elevated and can also have a cutaneous horn.[6] The cells at the base of these tumors show poor differentiation and consist of various sized masses of epithelial cells with pleomorphic nuclei, cellular keratinization, and atypical mitotic figures.[12] Difficulty in diagnosing these lesions often arises from an inability to determine the extent of superficial invasiveness of the tumor.

Keratoacanthomas are growths that are found on sun-exposed skin that usually initialize with rapid growth over a 2- to 3-week period without a pre-existing lesion. These solitary lesions appear as dome-shaped, red, smooth nodules, 1 to 3 cm in diameter, with a central keratinous plug that is lost, leaving a crater.[13] After a period of stasis, these lesions generally regress without treatment, often leaving scar tissue.[12] Because of the rapid and unpredictable growth of these eventually benign lesions, many specialists consider these as a subtype of SCC. Other types of non-melanoma skin cancers are derived from the other cell types found within the skin and include Merkel cell carcinoma, Kaposi sarcoma, cutaneous lymphoma, skin adnexal tumors and various other sarcomas. Because these types together account for less than 1% of skin cancers, they will not be covered further.

Pre-cancerous or pre-invasive skin conditions may be either early stages of skin cancer or may develop into skin cancer. Two such pre-cancers are of particular interest: actinic keratosis and Bowen's Disease. Actinic keratosis (AK) is caused by excess exposure to the sun and usually results in atypical epidermal cells in small, rough spots that may be pink-red or flesh-toned.[3] These lesions often appear in groups but have poorly-defined edges and can coalesce to form large patches. Most common in individuals with fair complexion, if untreated, these intraepidermal malignancies can

become SCCs.[5] The chromosomal abnormalities expressed in the presence of proteins (p53) and growth factors (Ki-67) show that this is a stage of neoplastic transformation. The rate of progression from AK to SCC is likely 0.1 to 10% over a lifetime.[14] The actual risk of subsequent lesion metastasis is between 2 and 6%.[15] Bowen's Disease (BD) or *squamous cell carcinoma in situ* presents as sharply marginated, erythematous, scaly or verrucous (wart-like) plaques with variable pigmentation.[12] These lesions are regarded as the earliest form of SCC, where the cells are still entirely located in the epidermis prior to dermal invasion.[3] Bowen's Disease is often similar in appearance to psoriasis with hyperkeratosis replaced with crusting, but the two lesions are sometimes indistinguishable.[13] Often a result of overexposure to UV radiation, BD may also be caused by HPV infection or exposure to inorganic arsenic.[12]

Due to the high variation observed in numerous different benign lesions of the epidermis, most of these cases will be ignored to focus on the most common lesion types. For further information regarding epidermal lesions and associated clinical features, pathologic findings, and differential diagnoses, please consider reference (12) listed below. Aside from the conditions covered previously, seborrheic keratosis (SK) and epidermal cysts comprise the majority of clinically observed non-melanocytic lesions.[12] Epidermal cysts are smooth, dome-shaped, freely-movable subcutaneous swellings. They are commonly walled-off cavities that are filled with keratin, derived from the hair follicle unit, and found on the face, neck or trunk.[13] These usually solitary lesions have been reported to rarely cause SCC, BCC, or BD.[12] Seborrheic keratoses are extremely common lesions that mimic both pre-malignant and malignant lesions and occasionally confused with pre-malignant or malignant melanocytic lesions. These common benign

keratotic skin growths increase in prevalence with age and are usually rough-surfaced papules, nodules, or plaques.[12] Because of the clinical variation presented, it is necessary for clinicians to understand the significant differences between these benign lesions and tumors. These pre-malignant lesions that can appear as highly pigmented tumors or varying size are commonly confused with the second major classification of cancerous tumors, malignant melanomas, which will now be considered in detail.

Malignant Melanoma

Melanomas are malignant lesions that begin formation within the melanocytes and, therefore, are most commonly hyperpigmented lesions. These lesions are widely considered to be the most serious type of skin cancer, originating in the epidermis but are much less common than SCC and BCC. Melanomas account for 65% of all skin related cancer mortalities, mainly due to the likelihood of metastasis when not detected early during development.[16] The presence of melanoma cells spreading to nearby lymph nodes may signify that cancer cells have reached to vital organs including the liver, lungs, or brain.[5] When detected at an early stage, like non-melanocytic cancers, melanoma can be treated with a high cure rate. Melanoma lesions can appear anywhere on the skin but often present on the trunks of males and the lower legs of females, or other sun exposed areas, especially the head and neck.[2] Because of the protection against harmful radiation that melanin affords, people with dark pigmentation are less likely to develop melanoma, but when it does occur, it is commonly found beneath fingernails or on the palms or soles of the feet. Unlike other cancers, melanomas are prevalent in young people as well, with 40% of cases occurring in people under age 50. The highest levels of incidence are still

found in the near age 55 range.[17] For patients diagnosed at age 75 or above, lesions are deeper and have higher mortality. These lesions can arise either directly from melanocytic growth or from pre-existing melanocytic nevi (moles). The most important prognostic factor for all melanoma lesions is the depth of invasion. Often because of the heterogeneity of clinical appearance, the melanoma can escape detection or be confused with other cutaneous lesions. Of greatest importance in distinguishing these lesions is consideration of a change in some aspect of the lesion, such as size, shape, color, or symptoms. Keeping the overall time-course of a lesion in mind, new or changing pigmented lesions in adults should be viewed with suspicion.[13] People that have had a melanoma in the past are also at increased risk of developing subsequent melanoma lesions in their lifetime.

As with the non-melanoma cancers, melanomas have associated benign tumors that must be well characterized for successful distinction during clinical diagnosis. Different types of these benign lesions develop due to proliferation of melanocytes and present as persisting macules, papules, plaques, and nodules. Such lesions can occur as the result of increases in melanin or melanocyte frequency within the cutaneous tissue. The benign lesions commonly associated with malignant melanoma are various nevi, including acquired, dysplastic, and congenital forms. These moles result from aggregation of melanocytes either at the epidermal/dermal junction, within the dermis, or both. As the name implies, congenital nevi are present either at birth or develop within the first two years of life, and commonly have 1 of 4 distinct histological types. They may have the distinct characteristics of nevus cells present in deep dermis (between collagen bundles) and subcutis, and infiltrate vessel and nerve walls of the deep dermis.[8]

Congenital nevi may be macular but often exhibit varied pigmentation and thickness, sometimes including the presence of hair. Another common presentation of nevi appears in the center of a de-pigmented zone, at which point they are classified as halo nevi. This condition is fairly common in young adults, characterized by the lack of melanin in the region surrounding a nevus, and is commonly caused as an immune response to a nevus. Depending upon the lesion, both the central lesion and halo can fade over time.[18] Acquired nevi are usually flat and small plaque, or dome-shaped papules or nodules. These usually increase in number until the third decade of life then decrease. Most commonly, these are relatively uniform and symmetrical in shape and color, but both of these traits can alter over time. Acquired nevi are common and alone do not pose a health risk. However, as the total number of acquired nevi increases, especially above 100, so does the risk of malignant melanoma. Dysplastic nevi have increased malignant potential, commonly pale-, red-, or tan-colored, appear early in life and in higher numbers than average. These are often larger in size, varied in color, shape, and contour, and are passed by autosomal dominant inheritance. Clinical features of note for dysplastic nevi can be found in Table I.3. The importance of the presence of a solitary dysplastic nevus, which is present in 5-10% of the US population, is unclear, but people with higher lesion counts have an increased risk of developing melanoma.[19]

Table I.3. Clinical Characteristics of Patients with Classic Dysplastic Nevi.[20]

Feature	**Clinical finding**
General clinical characteristics	
No. of nevocytic nevi	Often many **(>75)** including non-DN*
Uniformity of dysplastic nevi	Heterogeneous (neighbors differ)
Clinical characteristics of dysplastic nevi	
Size	Vary, but at least some over **7** mm diameter
Color	Variegate; multiple shades of tans, browns, black, red
Elevation	May be raised centrally
Perimeter	Fades imperceptibly into surrounding skin
Shoulder	Peripheral macular tan zone
Surface	Often mammillated (pebbly), cobblestoned
Location	Usually trunk > limbs > face
Change	Relatively stable once fully developed
Sun-exposed sites	DN greater numbers on sun exposed *versus* non-sun-exposed sites
Non-sun-exposed sites	DN greater numbers than non-DN*
Hypertrichosis	Absent
Symptoms	None
Erosion/ulceration	Absent

Current Diagnostic Methods

Early diagnosis for all classes of skin lesions requires regularly performed self-examination of the entire body. Because of the variability discussed above between lesion types, it is often most important for each person to know the groupings and patterns of lesion formation on their body and to be able to recognize new or expanding lesions. Specifically for potential melanoma lesions, the basic rule “ABCDE” can be helpful for evaluation of suspicious lesions: asymmetry, border, color, diameter, and evolution. Suspicious lesions will often appear asymmetric with a ragged or irregular border, exhibit variation in color across the lesion, have a large diameter of more than 5mm and the

appearance will alter over time, as demonstrated in Figure I.4. This rule helps during classification a suspicious lesion based on some of the criteria used to distinguish dangerous cancers. Once suspicious lesions are found, it is important to bring them to the attention of a health care professional for accurate diagnosis. The next step towards a diagnosis will include a medical history and physical examination of the lesions in question. Some dermatologists currently employ a technique called dermoscopy on patients to improve discrimination between lesion classes prior to an invasive biopsy. This technique relies on epiluminescence microscopy as a noninvasive method that allows the *in vivo* evaluation of colors and microstructures of the epidermis, the dermal-epidermal junction, and the papillary dermis, which are not visible to the naked eye. In the hands of an experienced clinician, some distinctions can be made between the melanocytic versus non-melanocytic and malignant versus benign nature of some lesions.[21] Early and accurate diagnosis of suspicious lesions is vital for medical care providers to mitigate excess stress for patients and dictates the treatment methods. In a study published by Stern et al, it was demonstrated that 49% of cases of seborrheic keratosis had a correct preoperative diagnosis.[22] While this is not pivotal for SK, which does not generally mandate lesion removal, such inaccuracy could be devastating for more severe lesions.

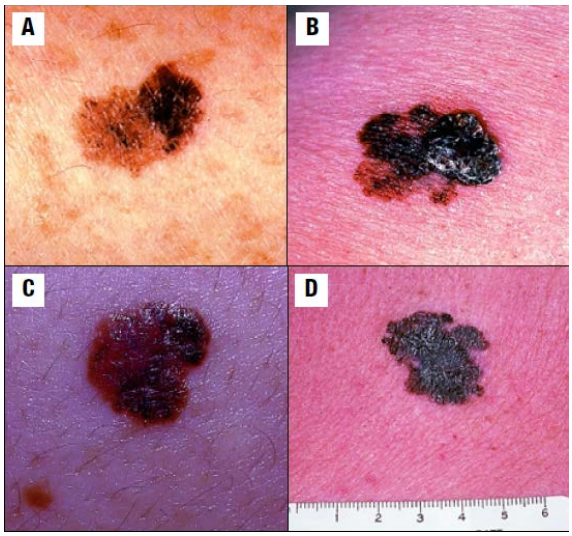

Figure I.4. The ABCD features of early melanoma. A) Asymmetry of early melanoma; B) Border irregularity of early melanoma; C) Color variegation of early melanoma; D) Diameter of early melanoma of approximately 2mm.[23]

If a lesion is considered suspicious after visual examination, a biopsy will be taken as the gold standard for proper diagnosis. This can be a shave biopsy, removing the top layers of epidermis and dermis with a surgical blade, a punch biopsy, to take a deeper sample through the epidermis, dermis and subcutis, or an incisional or excisional biopsy technique, corresponding to partial or complete removal of the lesion plus some tissue from deeper layers. For each of these options, the samples will be examined via microscope by a trained pathologist to determine status of the sample. For suspicious lymph nodes, special lymph biopsy techniques can be used to diagnose the potential spread of cancer as well, including fine needle aspiration biopsy, surgical lymph node biopsy, and sentinel lymph node mapping and biopsy. Cases of later stage melanoma with expected or possible metastases may employ imaging tests to assess the spread of cancer to lymph nodes or other organs. Common detection methods used for these

analyses include chest x-ray, computed tomography (CT), magnetic resonance imaging (MRI), positron emission tomography (PET), and bone scans, as listed in Table I.4.[2]

Table I.4. Comparison of Emerging Technologies in Melanoma Diagnosis.[16]

Technology	Sensitivity	Specificity	Advantages	Disadvantages
MoleMax	N/A	N/A	Two camera system; no oil immersion required; transparent overlay for follow up; total body photography	No computer diagnostic analysis
MelaFind	95-100%	70-85%	Multispectral sequence of images created in <3 seconds; Handheld scanner	-
Spectrophotometric Intracutaneous analysis	83-96%	80-87%	Diagnosis of lesions as small as 2 mm in diameter; observes skin structure, vascular composition and reticular pigment networks; handheld scanner	-
SolarScan	91%	68%	Empirical database for comparison; session, and image-level accuracy calibration; recorded on graphic map of body	Requires oil immersion
Confocal scanning laser microscopy (CSLM)	98%	98%	Histopathological evaluation at bedside with similar criteria; longer wavelengths can measure into papillary dermis; fiber-optic imaging allows for flexible handheld devices	Poor resolution of chromatin patterns, nuclear contours and nucleoli; can only assess to depth of 300 μm; melanomas without in situ component will likely escape detection
Optical coherence tomography (OCT)	N/A	N/A	High resolution cross-sectional images resembling histopathological section of skin; higher resolution than ultrasound and greater detection depth than CSLM	Photons are scattered more than once, which can lead to image artifacts; ointment or glycerol may be needed to reduce scattering and increase detection depth; observation of architectural changes and not single cells
Ultrasound technology	99%	99%	Cost effective; information about inflammatory processes of skin in relation to nerves and vessels	Tumor thickness may be overestimated because of underlying inflammatory infiltrate; melanoma metastasis cannot be separated from that of another tumor; images can be difficult to interpret
Tape stripping mRNA	69%	75%	Rapid and easy to perform; painless; practical for any skin surface; can retest same lesion	Results based upon small data set; delay in getting test results; need larger gene expression profiles for comparison; must send samples out for analysis (added cost)
Electrical bioimpedance	92-100%	67-80%	Complete examination lasts 7 minutes	Electrical impedance properties of human skin vary significantly with the body location, age, gender, and season

A novel detection method that is now commercially available and is under continued investigation for diagnosis of melanoma is MelaFind©. This small device uses multiple wavelengths of light to probe the tissue structures at multiple depths to develop a diagnosis based on quantified cellular assembly. While dermoscopy is the current standard of care, other new technologies to improve and aid diagnostic outcomes including the MoleMaxII© imager and SolarScan© use the same diagnostic algorithms, helping the physician to focus on particular aspects of a lesion before characterization. These new imaging-based technologies rely on high-resolution images of the lesions to help direct diagnosis within the clinical setting and are still under investigation worldwide, but they are generating databases for future diagnoses and are demonstrating the potential for improved diagnostic adjuncts for lesion differentiation.[22]

Current Treatment Methods

Treatment options for skin cancer depend upon stage, location, and classification of the disease, but most techniques are consistent across the disease type. The most common of these treatments include surgery, chemotherapy, immunotherapy, and radiation therapy. For most cases of skin cancer, surgical excision is the main form of treatment and is usually successful in curing early stage melanomas and most SCC and BCC cases. Thin lesions, including melanomas, can be cured using simple excision, which is similar to an excisional biopsy with the removal of a larger margin of healthy tissue to prevent local recurrence. The extent of this border depends upon thickness of each removed lesion. For small BCC and SCC, curettage and electrodesiccation are used to remove the cancer via scraping and coagulation of local tissue with electrode for repeated treatments. Microscopically-controlled or Mohs surgery is also common in SCC

and BCC. This process requires a surgeon to remove a thin layer of skin that the tumor may have invaded and to examine the whole layer under magnification for cancerous cells. If cancer is detected, the process is repeated until a layer is found lacking the presence of malignancy. This treatment is slow but tends to preserve normal skin near the lesion. There is some debate as to whether this treatment option should be employed for melanoma, requiring special tissue stains and no frozen sections, with concerns about recurrence.[2] Often, a sentinel node biopsy is performed by an oncological surgeon prior to a definitive procedure, limiting the need for a Mohs procedure.

More extreme cases of melanoma on the extremities or digits can require partial or total amputation to treat the cancer, but this is rare. For both SCC and melanoma, when the tumor has spread to nearby lymph nodes, the lymph tissue near the lesion can be dissected after a confirmed biopsy, but such procedures are rare due to associated complications. Early basal and squamous cell carcinomas are also commonly treated using other local methods including cryosurgery, photodynamic therapy (PDT), or local topical chemotherapy. Cryosurgery and curettage are common treatments for the pre-cancerous AK, of which cryosurgery is considered the standard of care.[24] PDT is less common for treatment of these cases due to the associated risk of damage caused by the photosensitizers for lesion targeting.[25] For metastatic melanoma cases, surgery is unlikely to cure the disease but is occasionally used to help control the extent of spread.

Systemic chemotherapy may be used to treat SCC and melanoma cases through the action of either injected or ingested drugs. Many such drugs are employed for each type of cancer and development of more efficacious alternatives is ongoing. Some of the recent and most promising options for melanoma chemotherapy treatment include

CTLA4 inhibitors (vemurafenib) to activate the immune response and BRAF inhibitors (ipilimumab) for the V600E BRAF mutation following mutation analysis. Attempts have been made to use cocktails of these drugs, as well as to localize the administration of the drugs to improve treatment outcomes. Studies suggest that combination chemotherapy is no more effective in treatment of metastatic melanoma than single-agent chemotherapy at increasing overall survival rates and is associated with more adverse effects than the single-agent counterpart.[26] Immunological treatment options involve the drug-induced activation of intrinsic immune responses to recognize and attack cancerous cells. These methods have shown effect in both non-melanoma (AK and BCC) and melanoma treatments. Examples include Interferon injection to boost immune response or application of Imiquimod cream, 5FU cream, or ingenol mebutate to stimulate immune response to cancer cells. Melanoma vaccines are under investigation in clinical trials, and BCC vaccine is used to stimulate the immune system by injecting a relative of the tuberculosis causing germ. Cytokines are proteins that boost the immune response upon injection and have been used for advanced stages of melanoma.[2] A new drug inhibiting the hedgehog signaling pathway (vismodegib) has promise for improved BCC treatment.

Radiation therapies have also been explored as avenues for the treatment of skin cancers. Lesions are targeted and treated using high-energy rays (x-rays) or particles (photons, electrons, or protons). The intense radiation treatment is common for large lesions or for patients that cannot tolerate surgery. This radiation therapy can potentially cure small, non-melanoma cancers, treat advanced stages of cancer or recurrent melanoma or metastases. Each of these treatments is associated with risks and side-

effects, so clinical options are determined with the help of a physician or health care professional depending upon the lesion status.

Optical spectroscopy

There are several drawbacks to current diagnostic methods for skin cancer. Most screening and diagnostic techniques rely on initial visual inspection, which can lead to false positives, and tissue biopsy, which is a subjective, slow, and relatively costly procedure prone to sampling error. Biopsy can also be painful and yields information only about a single location. Thus, there is a need for an accurate, real-time, non-invasive diagnostic tool. Optical techniques are particularly appealing for skin diagnosis because of the ease of access to the tissue of interest, the clinically relevant measurement times, and their potential for *in* vivo applications. Numerous optical spectroscopy techniques have been investigated as a potential solution to this diagnostic dilemma, particularly fluorescence, elastic scattering, and Raman spectroscopy.

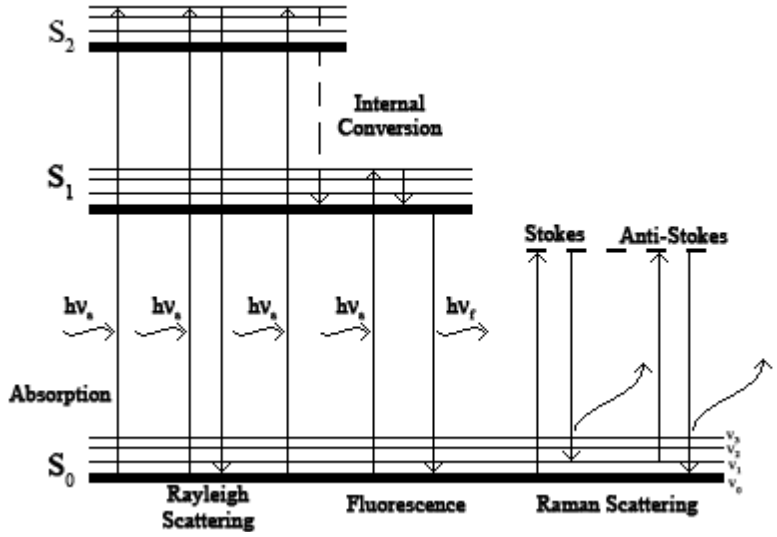

Figure I.5. Jablonski diagram illustrating principles of common optical spectroscopic phenomena. S_i denotes electronic energy state and ν_i refers to vibrational energy level. The horizontal dashed line represents a virtual excited state.

Fluorescence and diffuse reflectance

As shown in Figure I.5, fluorescence occurs when a photon is absorbed, heat is dissipated through internal conversion, and energy is subsequently re-released as a photon of lower energy. In tissue, autofluorescence signals from certain compounds like NADH, collagen, flavins, and porphyrins provide information about the metabolic or biochemical status of the tissue, and can be used to distinguish healthy and diseased states. Elastic, or Rayleigh, scattering is characterized by the change in path of an incident photon without losing or gaining any energy. This technique, also known as diffuse reflectance, provides morphological information about the tissue, such as number and size of scattering nuclei. Since these two techniques both have strong signals and provide complementary information, they are often combined to maximize diagnostic potential. Fluorescence and diffuse reflectance have been applied to cancer detection in

many areas of the body, including cervix [27-29], skin [30, 31], breast [32-34], and brain. [35, 36] The success these techniques have experienced in certain areas has been limited by their ability to distinguish among many different classes of disease due to the detected broad peaks.[37] This is especially true in the skin, where pigmentation and external chemicals can severely limit the penetration depth of the potentially dangerous UV excitation source.

Raman spectroscopy

Raman spectroscopy employs Raman, or inelastic, scattering. This occurs when an incident photon causes a scattering molecule to enter a virtual excited state and return to a ground state, which can be higher or lower than the original, through the emission of another photon, as seen on the right side of Figure I.5. Raman Stokes scattering occurs when the scattered photon has less energy than the incident photon, while Raman Anti-Stokes scattering occurs when the scattered photon has more energy than the incident photon. In contrast to fluorescence, which involves transitions between electronic energy levels, Raman scattering utilizes small transitions between vibrational energy levels. As this signal is less intense, a powerful laser source and sensitive detector is needed, as well as the removal of the much stronger fluorescence signal. A Raman spectrum is a plot of scattered light intensity versus the Raman shift of the scattered photon, resulting in sample information that is independent of excitation wavelength. The Raman shift is expressed in units of wavenumber, which is the reciprocal of the wavelength, and thus proportional to frequency. Spectra consist of a series of peaks, each of which represents a different vibrational mode of the chemical bonds or functional groups within a scattering

molecule. These peaks are narrow and highly specific to a particular bond, giving each molecule a unique spectrum from about 700 to 2000 cm^{-1}, or "fingerprint." Many biological molecules have distinguishable spectra, which can be used to determine the gross biochemical composition of a tissue from its Raman spectrum. One particularly relevant biochemical change previously discussed for cancer cells is an increase in the nucleic acid content concomitant with increased proliferation and genetic instability. This change, among others, can be detected with Raman spectroscopy.[38, 39]

Raman spectroscopy has historically been used in analytical chemistry to determine chemical structures or the presence of certain molecules, but has recently become a popular tool for studying tissue. This is largely due to the non-invasive and non-destructive nature of optical spectroscopic techniques, as well as the breadth of information that can be obtained from a single Raman spectrum. The majority of studies have been *in vitro*, attempting to distinguish normal from cancerous tissue in areas like cervix [40-43], breast [44-46], bladder and prostate [44, 47], lung [48], GI tract [44, 49], and the skin. Many have written of the challenges of bringing Raman to *in vivo* applications [50-52], but it has been successfully applied to cervix [53-56], GI tract [57-59], and breast [60]. Human skin, because of its ease of access, has seen a great deal of study by Raman spectroscopy. Earlier *in vitro* studies used mostly Fourier Transform (FT)-Raman to examine skin structure [61-67] and to attempt to distinguish normal from cancerous tissues.[68, 69] Due to the required integration times and instrumentation constraints, FT-Raman is not applicable for a clinical setting. An *in vitro* study used traditional Raman spectroscopy to distinguish BCC from normal tissue by producing two-dimensional Raman images.[66] Many *in vivo* studies have been performed as well, especially examining carotenoid content of the

skin[70-74], which is thought to play a role in defense against malignancy. Considering only the numerous reports of using fiber optic probe-based *in vivo* studies, many have investigated various structural and biochemical aspects of the skin[75-79], and several groups have used Raman spectra in combination with fluorescence or advanced multivariate statistical techniques to improve performance of discrimination between normal and cancerous tissues.[80-83] Recent reports have focused on clinical implementation of conventional fiber optic probe based Raman spectroscopy and reported distinctive spectra obtained from a large patient population.[78, 83] Despite these findings, practical concerns and independent validation are required before this technique can be widely implemented as a clinical tool.

As a stratified and heterogeneous tissue that is physiologically and optically complex, dermatological applications may have need of depth-resolved data. To this end, several groups have applied confocal Raman spectroscopy or Raman microspectroscopy to gather data from only a thin layer of the skin at a time. *In* vivo, these techniques have been applied to monitoring treatments [84, 85], determining molecular concentration profiles [61, 70, 86-91], and to discriminating between normal skin and BCC.[92-95] In our lab, previous studies have combined Raman techniques with other imaging modalities like optical coherence tomography and confocal imaging[96, 97], and used confocal Raman spectroscopy to distinguish among SCC, BCC, and non-normal benign tissues, like scar, when comparing the spectra to their respective normal spectra.[98, 99] Despite the numerous studies of skin with these and many other techniques, the previously mentioned changes to the tissue, the broad array of potential lesions, and its size have made fully characterizing and diagnosing these afflictions difficult.

CHAPTER II

ASSESSING VARIABILITY OF SKIN RAMAN SPECTRA

Introduction

Several research groups have reported using Raman spectroscopy (RS) to detect subtle changes in the skin related to wound healing, disease, natural moisturizing factor levels, protective antioxidants such as carotenoids β-carotene and lycopene, and cosmetics. The non-destructive nature of RS is ideal as an analytical or clinical tool for non-invasively monitoring the skin for changes associated with damage, disease, or treatment. Raman spectroscopy is sensitive to the biochemical composition of a sample without exogenous dyes, contrast agents, or extensive sample preparation. Because the underlying optical phenomenon is weak, the technology for *in vivo* skin measurement has only become available in the last 2 decades. Since the initial reports of human skin spectra in 1992, technological development and technique refinement have enabled *in vivo* Raman measurement. Studies have shown that spectra can be collected, corrected for undesirable signal components, and processed to rapidly provide feedback for users.[79, 100, 101] Previous reports have identified criteria required for adopting a novel biomedical diagnostic technique. In medical applications, many of these requirements are satisfied by RS for *in vivo* use: sensitivity to changes in tissue, application to *in vivo* studies, and novelty of information obtained non-invasively.[51, 52] However, standard Raman spectral databases are not available for tissue, limiting RS's role in influencing clinical decisions and patient prognoses. Both research lab and private industry studies using RS to

diagnose disease or understand tissue are becoming more common, but the RS community lacks a thorough understanding of the comparability of measurements made across multiple systems, tissue locations, and collection times.

Raman spectroscopy has been applied to the skin to study numerous changes. Skin is a complex and turbid tissue, with a layered structure, multiple functions, and inhomogeneous composition that can vary widely between patients and among various sites on a single patient. Several groups have demonstrated the feasibility of using RS to differentiate between skin malignancies and healthy tissues *in vitro*.[66, 69, 79] These studies also showed that different spectra correlate with specific skin disease types. Tissue components and structural conformations for several biomolecules related to skin function, including proteins, lipids, and carotenoids, have been determined based on Raman vibrations. These results have yielded new information about skin aging and structural properties that may differentiate disease types from normal tissues.[64, 70, 73] The healing of acute and chronic skin wounds has been monitored non-invasively with RS to provide new information on the biochemistry and progression of this complex process.[102-104] Benign conditions like psoriasis and atopic dermatitis, hydration differences, and the effect of topical treatments have also been studied using RS.[77, 105-108]

Current reports suggest that RS can be translated into the clinical setting with portable systems and fiber optic probes. However, as a clinical tool, RS measurements must be repeatable and free of confounding factors introduced by the system operator. With the probe-tissue interface of these systems, both contact pressure and probe angle can change, so the effects of user-induced variability must be understood and controlled. Other research groups have reported the effects of probe contact pressure on

measurements of diffuse optical spectroscopy and fluorescence spectroscopy in soft tissues.[109-112] Shim et al. reported no specific major spectral artifacts from contact pressure and probe angle on *in vivo* RS measurements during clinical gastrointestinal endoscopy.[59] To ensure that user perception of contact pressure and probe angle will not confound spectral measurements of the skin, the effect of each user-induced variability source will be isolated in this study.

Recent studies have demonstrated the effectiveness of RS for *in vivo* detection.[83] To our knowledge, previous reports include measurements made with a single instrument, thereby eliminating factors of instrumentation-induced variability. When limited to one instrument, however, multi-center studies or simultaneous data collection from multiple patients are impractical. Unlike other established medical tools, RS lacks standardized methods for system calibration, measurement, processing, data analysis, and reporting. Many Raman systems used in research are assembled from several vendors' components, and while core components remain the same, system response may vary. Reports on inter-device comparison and cross-validation studies of multiple medical instruments are available for other optical techniques such as confocal spectral imaging, dual energy x-ray absorptiometry, functional magnetic resonance imaging, and fluorescence spectroscopy.[113-117] The only report in using RS, by Rodriguez et al. addresses chemical analysis.[118] The consistency of pharmaceutical spectra measured across multiple devices suggests that reliable spectral libraries can be generated from Raman spectra of homogeneous samples. Measurements of tissues, like the skin, pose more rigorous challenges for cross-validation, as the tissue characteristics may vary between location and time of measurement. Raman spectroscopy of the skin offers

diagnostic potential because it can discriminate between subtle changes in normal, benign, and malignant tissues. If system variation is accounted for, RS can detect these subtle changes in skin. Using multiple RS systems during data collection will likely add instrument-dependent variables. If these variables are ignored, changes in the data may be incorrectly attributed to the samples measured instead of the devices used. The resulting potential decrease in sensitivity and specificity indicate the need for standardizing RS systems.

For skin, physiological variations may exist due to age, gender, race, measurement location, skin type, thickness, and hydration. Any of these patient variables could be used to distinguish or characterize measurements. Previous *in vivo* Raman studies have demonstrated depth-dependent changes in skin composition and anatomical location-dependent changes in natural moisturizing factor, which is a combination of amino acids and salts responsible for hydrating the outermost layer of skin.[61, 86] Knudsen et al. investigated variations in skin Raman spectra between persons, spots on the same body region, repeated measurements on a single spot, diurnal, day-to-day, and different levels of pigment.[65] In these reports, however, the authors utilized either Raman microspectroscopy, which has different instrumentation considerations than probe-based techniques, or Fourier-Transform Raman Spectroscopy, which has practical limitations for clinical efficacy. Along with the differences between techniques, the reports do not consider the influence of multiple instruments.

The goal of this study is to examine potential sources of variability for *in vivo* RS of skin and to suggest steps for limiting the influence of confounding factors to standardize Raman for clinical applications. The effects of contact pressure and probe

angle were characterized as potential user-induced variability sources. Similarly, the instrumentation-induced variability was also analyzed on skin and a non-volatile biological analog. Physiologically-induced variations were studied on multiple tissue locations and patients. The effect of variability sources on spectral line shape and dispersion were analyzed using statistical methods. In this study, *in vivo* measurements were made on healthy human skin with four stand-alone fiber optic probe-based RS systems. This manuscript reports the results from this study of influential variability sources when comparing Raman spectral measurements.

Materials and Methods

Instrumentation, data processing, & statistical analysis

Raman spectra were acquired using RS systems with similar optical components. Four unique RS systems were used as described in Table II**.1**. Each instrument was controlled by a laptop computer. A custom fiber optic probe consisting of 7 collection fibers (300 μm), without beam-steering modifications, surrounding a central excitation fiber (400 μm) was used to deliver 80mW of power to the sample surface. The tissue was cleaned with an alcohol swab prior to the initial spectral measurement. Spectra were collected with a 3 second acquisition time with the room lights and computer monitor turned off.

Spectral calibration was performed for each system independently using a neon-argon lamp with naphthalene and acetaminophen standards to correct for day to day

variations. A National Institute of Standards and Technology (NIST)-calibrated tungsten lamp was also used to account for the wavelength-dependent response of the instrument. The spectra were processed for fluorescence subtraction and noise smoothing using the modified polynomial fit and Savitzy–Golay methods, as described previously.[100]

Table II.5. Raman Spectroscopy system components utilized for multiple system comparison.

System	Fiber Optic Probe	Excitation Source	Spectrograph	Detector
1	7x1 fiber optic probe (EmVision LLC, Loxahatchee, Florida)	785nm laser (Process Instruments, Inc., Salt Lake City, Utah, PI-ECL-785-300)	Holospec f/1.8i imaging spectrograph (Kaiser Optical systems, Ann Arbor, Michigan)	Pixis 256BR CCD camera (Princeton Instruments, Princeton, New Jersey)
2	7x1 fiber optic probe (EmVision LLC)	785nm laser (Innovative Photonics Solutions (IPS), Monmouth Junction, New Jersey, I0785MM0350MS)	Acton LS 785 imaging spectrograph (Princeton Instruments)	Pixis 400BR CCD camera (Princeton Instruments)
3	7x1 fiber optic probe (EmVision LLC)	785nm laser (IPS, I0785MU0350MS)	Holospec f/1.8i imaging spectrograph (Kaiser)	Newton DU920-DR-BB CCD camera (Andor Technologies, Belfast, Northern Ireland)
4	7x1 fiber optic probe (EmVision LLC)	785nm laser (IPS, I0785MM0350MS)	Holospec f/1.8i imaging spectrograph (Kaiser)	Pixis 256BR CCD camera (Princeton Instruments)

Data analysis was performed on the spectral range 900-1800 cm^{-1}, a spectral region rich with information from proteins, lipids, and other tissue constituents.

Following data processing, each spectrum was normalized to its mean spectral intensity across all Raman bands to account for intensity variability. This normalization method was chosen to ensure that all wavenumbers retained statistical independence, which is required for statistical analysis and is compromised when spectra are normalized to the intensity of a single peak. Statistical analysis was performed on the data at each relative wavenumber. An Analysis of Variance (ANOVA) model was used at each wavenumber to separate groups and calculate appropriate confidence intervals. To quantify the changes in spectral dispersion between groups of measurements, two metrics were defined: total spectral variability ($TSV = \sum_{i=1}^{n} \sigma_i$), or the sum of calculated standard deviation (σ) at each relative wavenumber i across the entire spectrum, and total coefficient of variation ($TCV = \sum_{i=1}^{n} CV = \sum_{i=1}^{n} \sigma_i/\mu_i$), or the sum of the coefficient of variation (CV) at each wavenumber where CV is the standard deviation divided by the mean. The TSV is an absolute measure, indicating the combined dispersion in the measured data. The TCV is a measure of spectral dispersion relative to the data mean. Samples with low variability would have TSV and TCV values approaching zero, indicating reproducible and consistent spectral measurements.

Patients and Samples

Since inter-patient differences have been previously addressed by Knudsen et al., volunteers were of similar age and skin pigmentation with no history of skin disease; measurements were obtained from multiple, visibly-normal locations avoiding hair follicles, nevi, and other dark spots. Because skin is a potentially variable standard that undergoes continuous changes in hydration, a non-volatile biological analog was also

measured in each study to standardize spectral measurement and comparison. In this manuscript, generic intact vitamin E gel capsules were chosen as a homogeneous sample to isolate the impact of each variable, independent of tissue changes. Vitamin E gel capsules were chosen because they have several Raman scattering bands of varying intensity within the fingerprint region. Its peaks are broader than other drug formulations and measurements exhibit broad fluorescence signal likely due to the capsule composition (gelatin and glycerol). The layered composition and spectral traits of the capsules mimic the structure of skin and detected signals; accordingly, identical collection, processing, and analysis procedures were used to draw comparisons.

User-induced variability

Contact pressure and probe angle were the user-induced sources investigated. To isolate the impact of probe pressure, force values were quantified while five instrument operators applied probe pressures at three different levels. Raw chicken breast, used as a skin phantom, was placed on a calibrated scale, and the force applied by each operator was recorded as the operator held the probe in contact with the tissue for 3 seconds. The contact pressure tests were repeated at arbitrarily defined low, medium, and high levels, as perceived by the user. For these tests, operators were instructed that low pressure should minimally indent the skin surface while maintaining contact for the duration of the simulated measurement. Similarly, high pressure should simulate firm, stable contact with tissue that deforms. Subsequent RS measurements were made by a single operator with calibrated weights attached to a fiber optic probe mounted in a uni-axial stage, as previously described.[112] Spectra were acquired while applying different pressures at

levels encompassing the range of values observed during the probe operator tests. The effect of the angle between the tip of the probe and the tissue surface was examined by incorporating a rotational stage into the previous setup. Replicate measurements were acquired by a single operator in 2° increments up to ±10° from normal. For consistency, all measurements of the skin were obtained from the volar surface (palm side) of the forearm.

Instrumentation-induced variability

System stability was investigated for drift between collections and measurement repeatability after probe replacement. For measurement repeatability across time, measurements were made from vitamin E and a 1 cm^2 region of skin on the inner surface of the forearm. Measurements were made by a single operator over the course of 1-1.5 hours at 10 minute intervals in 2 sets over the course of a single day. A uni-axial translation stage held the probe in gentle contact with the sample controlling for pressure and angle. Six time points were collected in the morning and 9 more in the afternoon. For probe replacement, the uni-axial translation stage was used to measure skin and vitamin E controlling for contact pressure and angle of incidence. Repeated collections were acquired with the probe in contact with the sample. Subsequent measurements were made after the probe was translated away from and back into contact with the sample to mimic a controlled replacement of the probe and limit any photobleaching effects.

The performance of the 4 different systems was assessed through measurements of both the skin and vitamin E. Measurements were made of the skin using the systems

listed in Table II**.1**. All measurements were obtained in a single room on a single afternoon to control for temporal or environmental effects. Contact pressure and probe angle were controlled, and visible superficial blood vessels were avoided during probe placement.

Physiologically-induced variability

The measurements obtained with each of the 4 systems were repeated on 2 volunteers at multiple anatomical locations. The 5 skin sites measured were: 1) crease in index finger, 2) base of palm, 3) inner surface of forearm, 4) outer surface of forearm, and 5) cheek. In addition, measurements were also made on the inner surface of the forearm above and adjacent to a visibly-appearing large superficial blood vessel to probe the effect of subsurface blood vessels on the acquired spectrum. All measurements were controlled for temporal and environmental variables, as well as for contact pressure, probe angle, and the presence of visible superficial blood vessels. The biological analog was measured with each RS system for reliability analysis. Data was processed as described above.

Results

User-induced variability

Figure II.1 illustrates the influence of low, medium, and high pressure levels on RS of the skin. Significant differences were found between forces applied by probe

operators and between pressure levels applied ($p<0.0001$) using a 2-way ANOVA, Figure II.1a. However, significant differences were not detected between low and moderate pressure levels. The applied pressures, which were subjectively determined by each probe operator, exhibit large standard deviations for each of the three levels. Raman spectra (n=120) were acquired from normal skin at 22 different force values spanning the 3 pressure levels listed in Table II.2. The resulting spectra exhibit many visual similarities (Figure II.1b) as peak positions remained constant across test parameters, but intensities varied. Statistical analysis determined that fewer than 2% of wavenumbers were significantly different between low and medium pressures at the 95% confidence level, indicated by asterisks in Figure II.1b. By comparison, over 67% of wavenumbers significantly differed between high pressure versus medium and low pressure levels at the same confidence level.

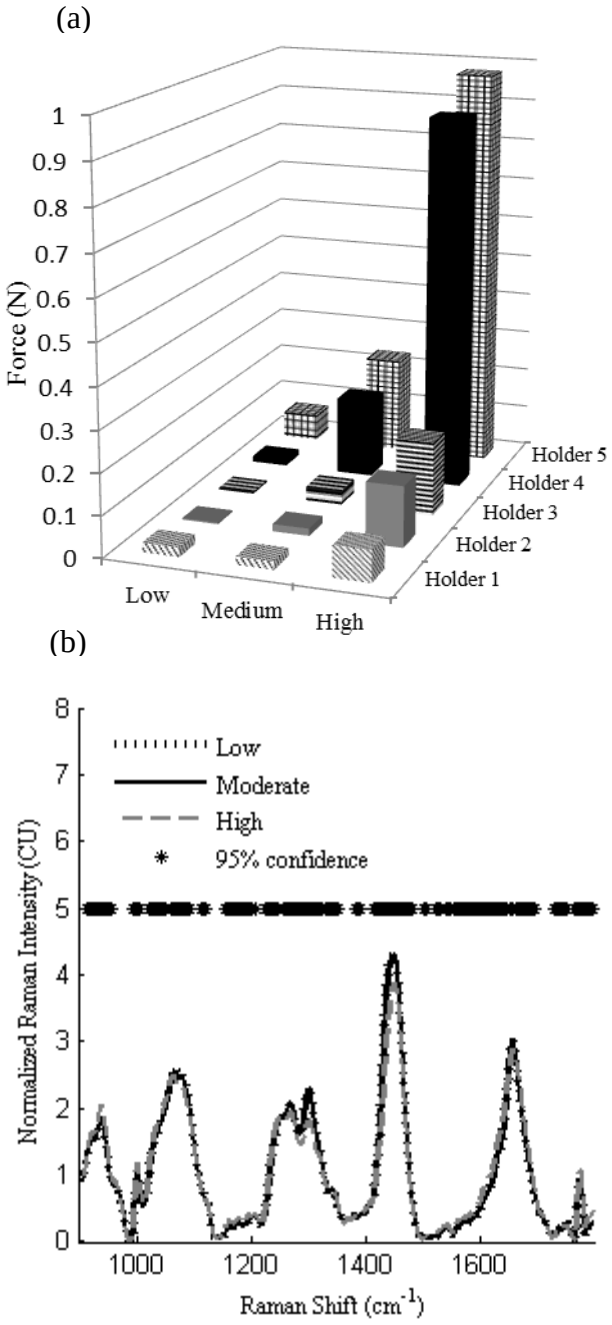

Figure II.6. (a) Averaged forces applied by probe operators during RS collection. (b) Raman spectra acquired from healthy normal skin (volar forearm) during application of probe pressure. Stars indicate statistical difference between high pressure and other measures.

Table II.6. Contact force (mean and standard deviation) applied by multiple probe operators

Low	22.3±28.6 mN
Medium	99.2±103.9 mN
High	457.8±425.5 mN

Randomized replicate Raman measurements (n=150) were compared at 11 different angles on the inner surface of the forearm accounting for normal (n=50), counter-clockwise (n=50) and clockwise (n=50) changes in the probe angle. The differences in probe angle had minimal impact on the obtained spectra. Mean spectra from each group displayed minor changes in peak intensity. Significant differences between groups occurred in fewer than 5% of wavenumbers (data not shown).

Instrumentation-induced variability

In this study, Raman spectra (n=15 for each) of vitamin E and the five anatomical locations on two healthy volunteers were obtained on the four different RS systems. Mean results from the biological analog and one location (cheek) from a single patient are presented for each RS system in Figure II.2 a and b, respectively. The skin spectra obtained were visibly similar and reproducible with minor variations in peak intensities. Significant differences ($p<0.05$) were found among systems at over 50% of the wavenumbers after system calibration and spectral processing, which was observed across all tissue locations measured.

To test for system stability between measurements, Raman spectra (n=15 replicates for each) were acquired from skin and vitamin E at 15 times over the course of

a day. Spectral shape and intensities were reproducible and consistent with the results obtained from 4 different systems. However, changes in spectral intensity of the skin resulted in significant differences ($p<0.05$) for over 50% of wavenumbers after calibration and processing. Measurements for probe placement were compared with measurements after the probe was replaced at nearly the same location via the uni-axial translation stage. After replacement, 5% of wavenumbers significantly differed between the groups for skin (data not shown).

To confirm that the observed variations between spectra were associated with the skin sample, vitamin E was measured during each study protocol. For all variables considered, including contact pressure, angle, repeatability, probe replacement, and measurements made across systems, there were no systematic differences between vitamin E spectra. For example, as quantified in Table II.3 and depicted in Figure II.2a, vitamin E spectra acquired across systems after data processing were completely reproducible. Measurements by a single system are expected to have a low total spectral variability, TSV, and low total coefficient of variation, TCV. When the data collected from multiple systems are pooled prior to calculation, the TSV and TCV give an indication of the absolute and relative dispersion induced by data collection with multiple systems. A single system had at most a TSV of 3.7 and a TCV of 22.5 for vitamin E and a maximum TSV of 14.4 and TCV of 57.2 for a single skin location. The pooled data across all systems for vitamin E had a TSV of 11.1 and TCV of 29.4, while the pooled measurements on a single skin location resulted in a TSV of 45.2 and TCV of 98.2. For both individual system and pooled calculations, the values for a single skin location are higher than for vitamin E. The greater values for skin compared with vitamin E suggests

that detected changes are primarily the result of the sample and not the system. Comparison of a single system and pooled data for vitamin E suggests a high level of overlap in the measurements obtained by different RS systems, while more complex interactions are associated with the skin.

Table II.7. Quantified spectral variability for skin and biological analog for individual RS systems and pooled data.

Sample	**System**	**TSV (AU)**	**TCV (AU)**
Vitamin E	1	2.149358	16.41168
	2	2.533614	22.1533
	3	3.725334	22.5385
	4	2.501374	20.02703
Single Skin Site	1	13.19235	34.58927
	2	14.36957	57.2284
	3	11.73376	45.67666
	4	14.23391	52.98108
Vitamin E	All	11.1398	29.4302
Skin Site	All	45.20325	98.18677

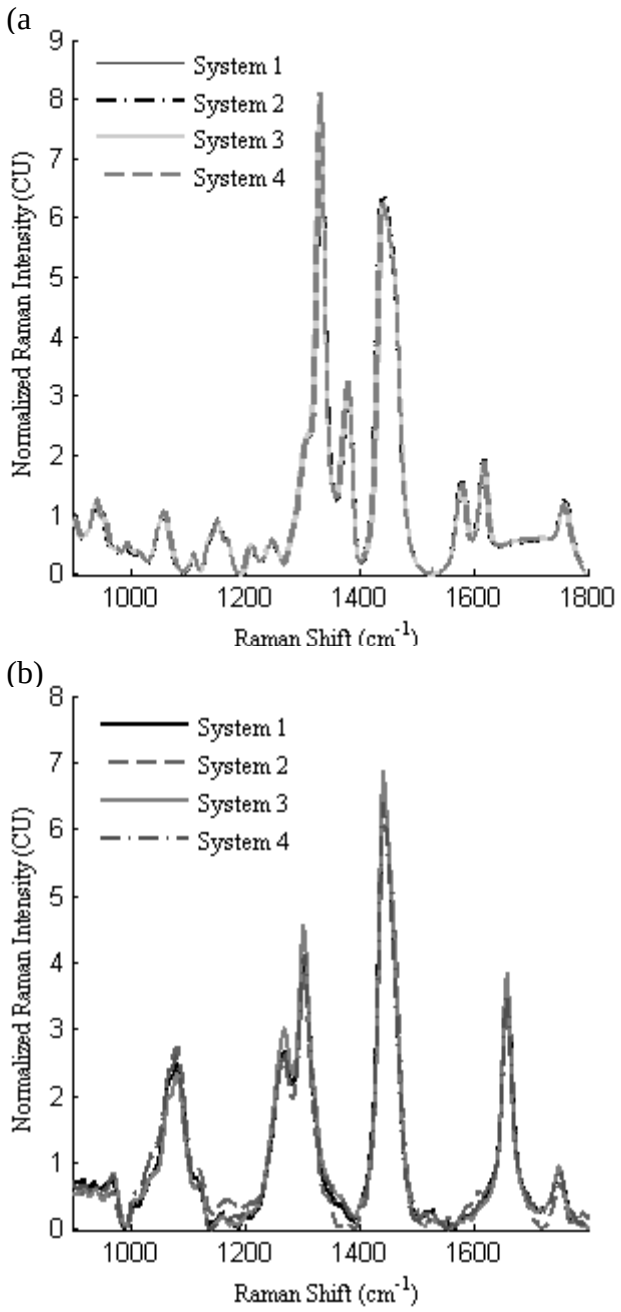

Figure II.7. (a) Raman spectra of Vitamin E as a biological analog measured by 4 RS systems. Identical signals were obtained after uniform collection and processing algorithms used. (b) Mean Raman spectra (n=15) of one skin site measured by 4 RS systems.

Physiological-induced variability

Raman spectra (n=15) were obtained from each of 5 anatomical locations on the upper extremity and face from 2 healthy volunteers. Based on the results, substantial intra-patient differences are present between unique anatomical locations (Figure II.3a). Measurements made were repeatable across days and patients for each location. The peaks with intensity variations have previously been correlated with tissue protein and lipid content (1440 cm^{-1} and 1750 cm^{-1}) and Amides I (1645-1680 cm^{-1}) and III (1230-1300 cm^{-1}).[119, 120] The spectra group together into spectral families, each having a unique line shape. For example, there are few variations between the spectra acquired from family 1, the finger and palm, but these variations are not consistent with the few variations between family 2, the face and both sides of the arm. As quantified in Table II.4, when all the data from the 5 sites across a single system are pooled, the TSV is 55.1 and TCV is 92.8. When separated into the two families described above, the values decrease. Combined spectra from the arm and cheek result in a TSV of 29.7 and a TCV of 70.6. The finger and palm spectra have a TSV of 26.3 and a TCV of 62.0 when combined. When a single location was considered the values were lower still, with a maximum TSV of 17.6 and a TCV of 54.5. The decrease in TSV and TCV indicate consistent spectral families when the data is grouped. The families differ in peak intensities at 1440 cm^{-1}, the presence of defined peaks at 1300cm^{-1} and 1750cm^{-1}, and the full width at half maximum (FWHM) intensity of the Amide I band centered at 1658cm^{-1}.

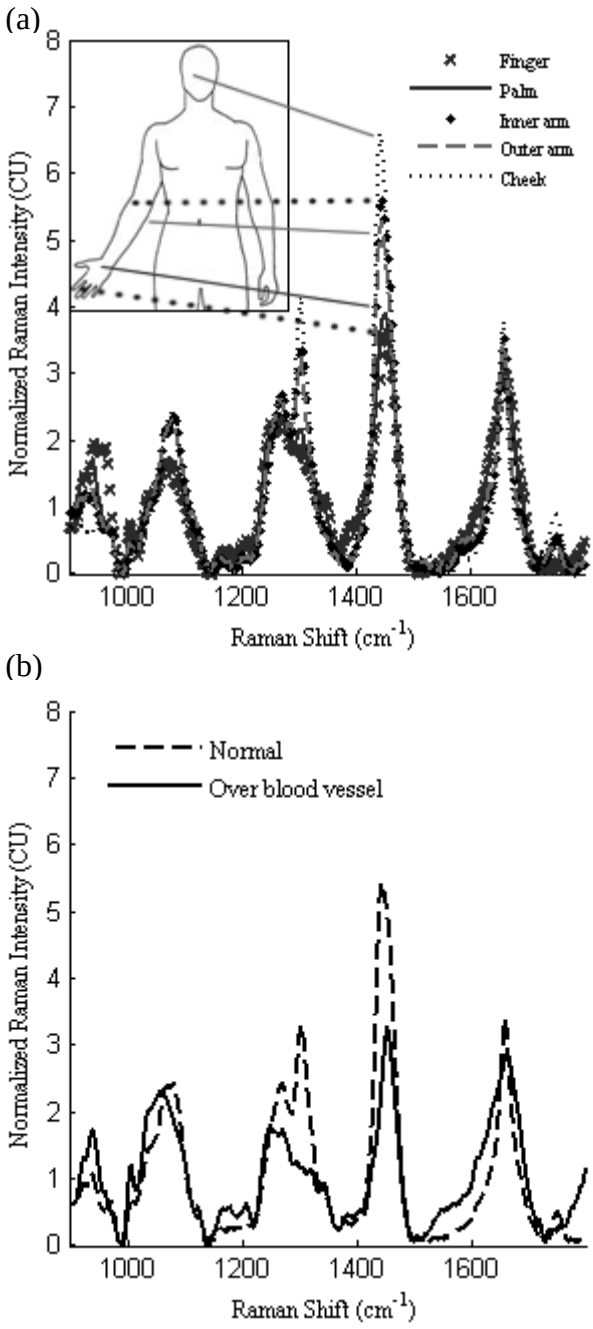

Figure II.8. (a) Intra-patient location based differences in Raman spectra. (b) Raman spectra acquired from healthy skin above and adjacent to a large superficial blood vessel.

To evaluate the effect of superficial blood vessels beneath the sampling volume of a normal measurement, Raman measurements (n=15) were obtained from normal tissue

directly above a visible vein and adjacent to the same vein. As Figure II.3b shows, there are changes in spectral signatures including notable spectral disintegration from 1200-1300 cm^{-1}, decreased intensity at 1440 cm^{-1}, and a broader 1658 cm^{-1} peak, which are all reproducible for measurements above a vessel. When comparing the normal measurements obtained from skin over the vessel in Figure II.3b to the spectra in Figure II.3a, the measurements over a vessel on the forearm more strongly resemble spectral family from the finger than the forearm itself. Grouping spectra from above the vein with those from the adjacent forearm resulted in a TSV of 62.5 and TCV of 91.4, compared to the TSV of 50.6 and TCV of 80.1 when grouping above the vein and finger spectra, which has no obvious meaning.

Table II.8. Quantified RS single system variability for skin sites grouped into spectral families and pooled data.

Grouping	**TSV (AU)**	**TCV (AU)**
All skin sites	55.09592	92.83188
Family 1	26.3364	62.00486
Family 2	29.72205	70.62611
Single Skin Site	17.62649	54.46361

Representative mean spectra from multiple systems for 2 locations on a single patient are presented in Figure II.4. Each location retains the unique spectral signature measured and presented in Figure II.3a for the finger (site 1) and the cheek (site 2), but measurements from individual systems contribute characteristic variations to the data. With differences in filtering and tissue fluorescence, the spectral response calibration and signal processing for background removal was unequal between systems and anatomical

locations. Despite the systematic effects on data collection by each instrument, the data still group consistently into spectral families with similar line shape.

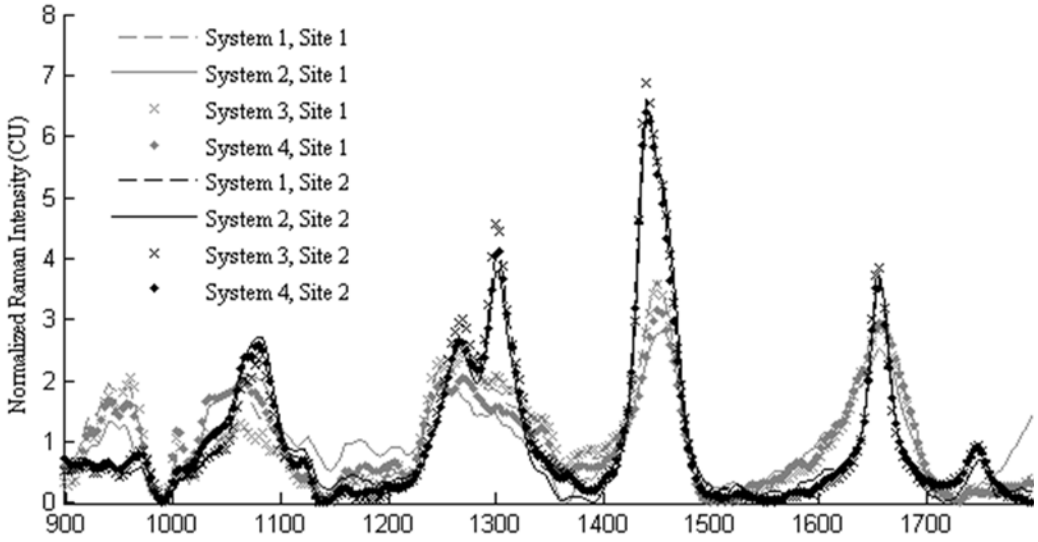

Figure II.9. Raman spectra from 2 anatomical locations on a single patient measured on 4 RS systems.

Figure II.5 extends the previous analysis to include multiple patients and depicts spectral changes associated with locations on multiple patients measured with different systems. The results strongly mirror those of multiple locations on a single patient, where strong location- specific signals are present and repeatable between patients and system based changes impact each measurement similarly. Measurement from a single location resulted in consistent spectral line shape between patients and systems. However, the intensity of acquired spectra differed between patients and between systems. This is most clearly depicted in Figure II.5 by the grouping of site 2 measurements. Also, the intensities for spectra from patient 1 are grouped compared to the spread of patient 2

spectra. This effect is most obvious at the peak intensities for 1440 cm^{-1} (CH_2 bending) and 1300 cm^{-1} (Amide III CH stretch).

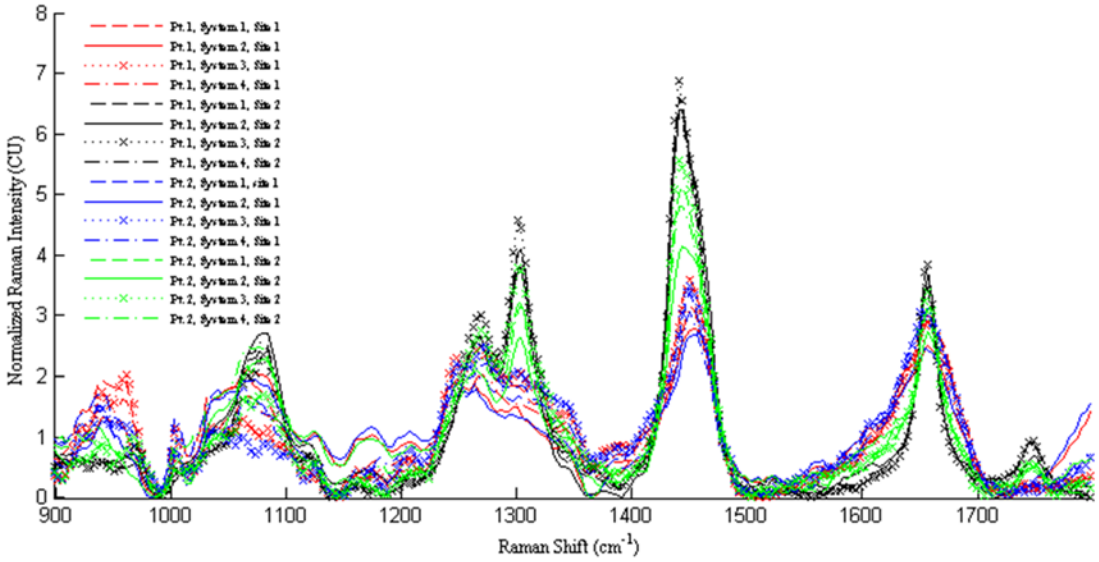

Figure II.10. Raman spectra of 2 anatomical locations reproduced for 2 patients measured on 4 RS systems.

Based on the ANOVA analysis presented in Figure II.6 for the complete block design of measurements made from 5 locations on 2 people with 4 instruments, the intra-patient variation ("Location") is the most influential factor. The inter-patient differences in the spectra account for less than 8% of the variance from the entire dataset. This value was minimized by controlling for inter-patient variables prior to the study. The inter-patient differences were insignificant compared to 28% contribution from system and 42% from location. The interaction between inter-patient and intra-patient differences is consistent with the patient specific changes presented in Figure II.5.

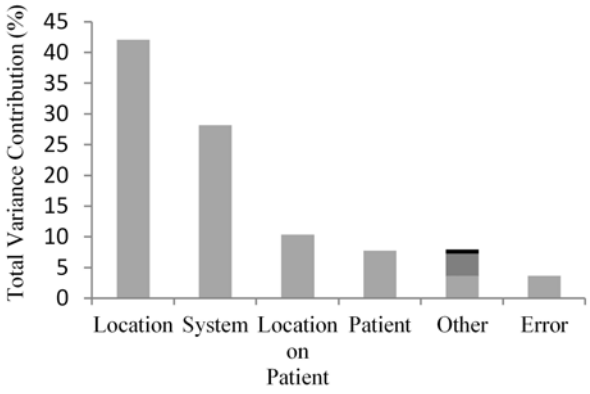

Figure II.11. Percent contribution by source and interaction terms to the variance of RS data. The presence of the Location on Patient interaction term indicates that a location may take a unique intensity level for each patient measured. Non-significant interaction terms are combined in Other and represent less than 8% of total variance.

Discussion

Previous studies have investigated the use of RS to detect changes in skin, but few have addressed the latent sources for variability during measurement or the potential issues when comparing biological measurements between systems. The initial goal of this study was to understand how different sources of variability impact the measured Raman spectra of skin. An obstacle to testing these variables in tissue is the inherent inconsistency and sample inhomogeneity. To avoid this innate biological variation, a biological analog, vitamin E, was introduced. In this paper, Raman spectra acquired from both normal tissue and vitamin E are evaluated for the effects of three broad categories: user-induced, instrumentation-induced, and physiologically-based sources of variability.

User-induced variability

As a new and increasingly-used clinical tool, RS users need to understand the impact of contact pressure and fiber probe angle on obtaining consistent and accurate results regardless of the user. Analysis in this study found no significant differences or increased variability introduced when user-induced factors were properly controlled. Even with high variability in the subjectively determined pressure exerted by different probe operators, demonstrated in Figure II.1a, spectra with low variability can be obtained. The results of applying varying pressure during spectral measurement suggest that a range of applied pressures are acceptable for collecting reproducible and reliable Raman spectra (Figure II.1b and Table II.2). Spectral change was observed only in measurements made under high pressure, in this case over 111kPa. Previous studies have shown that increasing pressure can change the interactions between light and tissue, for example by decreasing fluorescence and increasing optical penetration depth.[21-23, 34] Increased probe pressure will compress the tissue and more densely pack Raman active molecules, potentially leading to more frequent Raman scattering events. Likewise, increased pressure could lead to occlusion under the tip of the probe, altering perfusion and blood content within the sample. The acceptable range of applied pressures may depend on variable thickness, hydration, elasticity, or other patient, location, or age related changes. In general, however, the probe should minimally or reversibly displace the tissue surface and remain in contact during the measurement. The increased variability introduced by high contact pressure can be avoided if users are trained to operate under low pressures. These findings may also allow for better measurement comparison, if changes in penetration depth, perfusion, and autofluorescence are desired.

By changing the angle of contact between the probe and sample, the volume of tissue being measured will change as the light scatters. Despite this subtle change in interrogated tissue, few significant spectral differences were collected between signals over the range of measured angles. The sampling volumes of fiber-optic probes are relatively large compared with tissue structures, yielding a low probability that a slight variation in probe angle will cause dramatic changes in the spectrum. However, because probe collection geometries have many designs, slight variations in probe angle may collect signal from a different location than intended. Probe operators should understand the importance of using consistent angles between measurements.

Instrumentation-induced variability

The common practice of using a single instrument during data collection has had both positive and negative consequences for RS. While it has simplified data interpretation for researchers by removing a significant variable, it has also hindered both data comparison and spectral database development, which are prerequisites for generating reliable diagnostic algorithms. In this study, the contribution of instrumentation-induced variability to the acquired spectra was validated and quantified for several potential sources. Variability between repeated measurements for time points and probe placement was found to be insignificant, confirming previous reports.[65] During Raman measurements, instrumentation-induced variability was considered a system dependent response. This is demonstrated in Figure II.2b, where minimal intensity differences between systems were detected within a single location of the skin. These small differences were obtained after spectral response calibration, processing, and

normalization, which are important steps in reducing differences between instruments. However, these steps alone may not be sufficient to remove the effects of multiple instruments and probes. Spectral response calibration accounts for only the detection arm of an RS system and requires system isolation for calibration, which is impractical in a clinical setting. Other data processing options are currently under investigation. Because probe-based RS systems can have variable components, calibration methods need to account for the specific and collective responses of the system. Several research groups, including ours, have proposed the use of reflective standards or other similar calibration techniques that account for both excitation and collection branches of the system to address and potentially minimize these responses. When comparing spectra from a single location measured by multiple systems, as presented in Figure II.2, there are no significant differences. However, comparing spectra from a different tissue location or patient (Figure II.4 and Figure II.5), these signals are complicated by other factors.

Isolating system dependent responses with vitamin E also generated negligible differences in spectra acquired by different instruments after processing. The narrow range of detected Raman signal for the biological analog, depicted in Figure II.2a, confirm the instrument stability and reliability which is needed for cross-validation and spectral library generation. After investigation of numerous vitamins and organic products, including vitamin B12, fish oil, and coffee, vitamin E was chosen as the best mimic for soft tissue signals. As the interrogated sample becomes more heterogeneous, the complex interactions of inherent scattering and system-dependent response increase spectral variability. This result is demonstrated in Table II.3, where the TCV for vitamin E of separate systems are approximately equal to the pooled value for all systems. In

contrast, the TCV for skin of separate systems are half the value for the data pooled for all systems, demonstrating that the complexity of skin results in increased variability that differ between RS systems. For measurements made with separate RS systems, users must understand the implications for cross-system comparison and determine how spectral changes introduced by separate instruments will influence the diagnostic capability of an algorithm. Using a biological analog can aid in evaluating multiple RS instruments for consistent measurement and comparison of tissue spectra.

Physiologically-induced variability

Variability sources based on characteristic tissue differences between multiple locations on a single patient and between patients were identified as important factors for RS of the skin. The anatomical location analysis yielded spectra with visibly and statistically significant differences (Figure II.3). This result is consistent with anatomical knowledge of the diverse heterogeneity of skin. Multiple studies have documented the anatomical location-based changes in many skin properties including thickness, presence of hair, tissue hydration, pigmentation, sun exposure/damage, subsurface structures, and compositional differences of lipids and proteins.[64, 121-123] Raman scattering signals from different anatomical locations are distinct, so tracking where such measurements are made is critical when comparing across locations. Separating the anatomical locations into distinct spectral families, based on intensity and line shape as in Table II.4, may be a more thorough comparison of physiologically-induced changes that are not directly caused by variations in the measurement location.

Statistical analysis reveals that the spectral variance and primary source of variability depends on peak intensity. TSV is dominated by fluctuations in peak intensity of major Raman active bands, with 1440 cm^{-1} (CH_2 bending) accounting for nearly 30% of total variability in the data and 1300 cm^{-1} (Amide III CH stretch) for another 10%. Physiologically-induced variability, due to measurement location, dominates the dispersion sources when comparing multiple anatomical locations for a single system and appears at strong Raman peaks. Instrumentation-induced variability dominates regions of peak shoulders and background subtraction when comparing a single measurement location across different systems.

Significant spectral differences were also observed between patients (Figure II.5). Studies from our lab and others have reported the sensitivity of RS to patient-based variables.[65, 124] Some of the potential variables that may contribute to the observed inter-patient changes in spectral signature for normal healthy skin include hormonal variations, BMI, gender, race/ethnicity, age, accumulated photodamage/UV exposure, and pigmentation. Knudsen et al. reported significant peak intensity ratio differences between patients, which agree with findings presented here. In that report, a single location (buttocks) across 13 patients yielded mean values ranging from 0.94-1.15 for the intensity ratio of Amide I (1660 cm^{-1})/CH_2 bending (1440 cm^{-1}). The mean values measured between patients here ranged from 0.70-0.76 for this ratio. The differences between the reported peak ratios are likely the result of variations in study equipment and processing procedures, making comparative studies between institutions difficult. However, the variation in values is consistent between reports, indicating inter-patient changes detected in the skin. Further analysis of our data suggests that these ratios are dependent upon

location of the measurement. The mean values obtained here range from 0.863 on the hand to 0.563 on the cheek of a single patient.

To simplify comparisons between patients, age and skin type were controlled. The inter-patient differences detected here demonstrate minor spectral changes when controlling for other variability sources. Physiological variability between locations within a single patient has been reported in the literature and suggests the need to account for anatomical site prior to comparison.[61] A potential method to overcome these variations would utilize paired spectral measures, or the collection of adjacent and contralateral normal measurements for each measurement of interest. Difference spectra between the variable and paired normal locations would normalize a measurement to its inherent location-based signal, which could remove influences of intra-patient variation. Selection of the location for a paired measurement is critical due to the location-based variability in signal. A further complication is introduced by the presence of superficial blood vessels beneath the measurement location. The obtained spectrum from atop the vessel neither replicates skin measurements nor the reported spectra of blood, suggesting that signal changes are not derived from the blood alone.[86] The results in Figure II.3b suggest that paired measurements should come from adjacent or contralateral locations of normal tissue, avoiding hair and visible superficial blood vessels. Adjacent measurements from the same small area of tissue were found to be reproducible, but the size of this area is unknown. In general, the closer the paired measurement to the original measurement location, the more likely a measurement will account for normal variations.

Statistical comparison indicated that anatomical location most significantly impacts collected data, followed by instrumentation-induced variability and inter-patient

changes (Figure II.6). These findings suggest that when patient variables are controlled the detected inter-patient differences exert less influence on the data than alternate sources. The significant interaction term ("Location on Patient") is likely the result of inter-patient variation that affects intra-patient changes. Each patient will have unique effects on the spectra that will cause individual anatomical location to vary in intensity. The presence of this interaction complicates the interpretation and impact of multiple patients. As all other interaction terms combined have little influence, it is logical to conclude that the primary concerns for spectral variability will be the effects from anatomical location, system, and patient based differences. These patient specific differences may become the dominant source as a more diverse population of normal tissues is analyzed. This result further emphasizes the need to control for the measurement location.

Because the influence of a particular source of variation is not uniform across the spectrum, understanding and minimizing variability sources is important. Through ANOVA of spectra at each wavenumber, the relative impact of each source of variability can be discerned. Spectral libraries and algorithms for diagnosis or tissue classification need to perform independently of these confounding variability sources. Algorithms may need to account for the variances introduced by multiple instruments or compare spectral regions that are dominated by a common variability source. For example, the intensity of CH_2 bending (1440 cm^{-1}) is dominated by physiologically-induced variability, while the FWHM of the 1070 cm^{-1} feature, which is linked in-part to silica fiber signal, is dominated by instrumentation-induced variability. A ratio of these features would give inconsistent and instrument-dependent results. The dispersion of strong Raman active

bands are associated with differences in anatomical location and should be used for intra- and inter-patient comparison. Comparing regions of background subtraction will represent variations between multiple instruments.

The purpose of this paper is to examine different sources of variability that can impact *in vivo* RS measurements of skin and to suggest steps for limiting the influence of these confounding factors. Table II.5 briefly outlines the sources examined and the influences detected. These results indicate that, when properly used, contact pressure, probe angle, and probe replacement have no significant contribution to spectral variance. The use of multiple RS instruments will undoubtedly introduce some variation into the collected data, but options to limit these influences are under investigation. Despite these findings, thorough analysis of the potential sources of measurement error should be conducted with any system to understand the obtained results, ideally prior to the beginning of the study. We suggest that several steps be taken during the design and execution of *in vivo* RS skin measurements to address potential sources of variability. These steps are as a follows: 1) Standardized tissue cleaning protocols, such as cleaning with an alcohol swab, should be used to minimize error contribution (especially for measurements of the face and hands due to cosmetics and lotions); 2) Measurements with the probe should use low but consistent pressure during collection, keeping the probe approximately normal to the surface (user should be trained); 3) For normal measurements, a single collection per location is sufficient; 4) Paired measurements may provide normalization of a spectrum to the inherent signal based on anatomical location and person specific signals; 5) The selection of the location for a normal paired measurement should be carefully determined, avoiding hair follicles and major

superficial blood vessels. Furthermore, adjacent and contralateral normal measurements at a single location should be investigated for consistency.

Table II.9. Variability sources investigated and determined effects.

Variable	**Effect**
Contact pressure	For low or medium pressure, no detected effect High pressure, significant effect detected
Probe angle	No detected effect
Probe replacement	No detected effect
Instrument stability	No detected effect for biological analog Significant effect detected between tissue measurements
Multiple instruments	No detected effect for biological analog Significant effect detected for biological samples
Anatomical location	Significant effect detected
Presence of blood vessel	Significant effect detected
Inter-patient	Significant effect; Minimized by controlling patient variables

Conclusion

In general, these findings apply to probe-based measurements for all optical modalities; other collection configurations, such as confocal microspectroscopy, will likely contain alternate variability sources to address. Practically, normal tissues are not often studied, as they are not the focus of a novel diagnosis or treatment. The default assumption is that all normal samples are similar; however, complex interrelationships and differences between separate normal tissues exist. By expanding our understanding of normal tissues and the influence of data collection and instrumentation, the potential exists for more accurate and effective analyses to differentiate unique variables of

interest. The analytic methods for RS should consider the major sources of variance contribution prior to the development of classification algorithms. Thorough analysis of instrument response, stability, and calibration are important to standardize RS as a clinically viable tool. Measurements by separate instruments will likely exhibit unique responses. If these variations are understood and accounted for, measurements can be compared across systems and spectral libraries can be compiled. Here, practical considerations and results are presented that suggest how RS, and other probe-based optical techniques, can and should be used *in vivo* to minimize sources of variation prior to processing, comparison, and classification, leading to an application that can be used to accurately differentiate disease classes.

CHAPTER III

FUTURE DIRECTIONS

For the first time, multiple fiber optic probe-based Raman spectroscopy (RS) systems have been evaluated for unique variability sources that impact *in vivo* measurement. The influence of user-, instrumentation-, and physiologically-induced factors were examined during measurements of normal healthy skin. Results of this study suggest that each of these categories include influential sources of variability that can impact the application of RS for *in vivo* measurement of the skin without proper control.

The influence of user-induced variables of probe angle and replacement had no significant effect on the acquired signal, but the application of high probe pressure resulted in altered spectral line shape. Instrument evaluation verified stability on a consistent biological analog (vitamin E), but *in vivo* spectra were found to differ significantly between measurements. Multiple systems also obtained consistent results between spectra of vitamin E, but influential effects were observed during *in vivo* measurements. Physiologically-induced variables for distinct anatomical locations, the presence of visible superficial blood vessels, and separate individuals all accounted for significant effects on the obtained Raman spectra *in vivo*. Despite these findings of significant effects of variability sources, further characterization and mitigation of relative impact is needed before RS of the skin can be successfully implemented and studied using multiple systems.

An interesting finding of the previous work was that consistent signals were obtained independent of the angle between the probe and tissue surface, within a controlled range. Continued investigation must assess whether this is valid for all probe designs or if unmodified fiber optic probes behave differently from different configurations. The impact of photobleaching must also be evaluated for impact on repeated measurements. Similar effects were observed during probe replacement tests, but were controlled for by allowing relaxation time between measurements. A thorough understanding of these user-induced variables will promote *in vivo* RS applications.

A primary limitation for use of multiple RS systems is the lack of understanding for comparing independent instruments. This was addressed in the research presented above, but must be investigated in greater depth. The observed spectral contributions of each RS system must be characterized as either a fixed or random effect. With this knowledge, potential calibration transforms may be generated to allow direct comparison of measurements made by separate systems. Further investigation of the reflective standard for spectral response correction is necessary to further reduce system-dependent responses. The influence of fiber optic probe collection-excitation geometry must be investigated to see if the design significantly changes the acquired signal. Based upon the possible differences in collection volume and depth interrogated, probe optimization is important to ensure that signals are consistent between collections when other parameters are appropriately controlled.

Further investigations that focus on the impact of physiologically-induced changes *in vivo* would build upon the study presented above. The observed signal changes between anatomical sites should be expanded to obtain a better understanding of

locations with comparable spectra. The underlying explanation for the signal change associated with visible superficial blood vessels is also not yet apparent. Potential reasons could be based on the change in interrogated tissue, which has more smooth muscle, vascularity, and collagen in the vessel wall. Also, serum protein and other blood components could explain some of the spectral changes, if the signal were acquired from the vessel itself. The comparison of interpatient variability should also be expanded to a larger and more diverse population, to assess age, gender, BMI, and other factors that were accounted for previously. Finally the influence of photodamage and aging, both natural and premature, should be investigated with RS to determine if significant spectral changes are associated with these variables as well.

Despite the focus of this research on the skin as the target tissue of interest, the issues addressed in this research study are applicable to optical diagnosis of other tissues and technologies. Understanding the numerous and varied sources of variability that are present within a system are vital when planning and conducting research and analyzing and interpreting results. Because the systems used by many researcher groups are experimental and often assembled rather than purchased intact, investigating and cross-validating results are necessary steps prior to the broad application to the research goals and target applications studied. The complexity of *in vivo* models and applications ultimately require precise control over experimental design to limit the error and improve accuracy and potentially, diagnostic outcomes.

REFERENCES

1. American Cancer Society., "Cancer facts & figures", (The Society, Atlanta, GA, 2012), p. v.

2. "Melanoma Skin Cancer", in *Learn About Cancer: Detailed Guide* (American Cancer Society, 2012).

3. "Skin Cancer: Basal and Squamous Cell", in *Learn About Cancer: Detailed Guide* (American Cancer Society, 2012).

4. A. Rook, D. S. Wilkinson, and F. J. G. Ebling, *Textbook of dermatology* (Blackwell Scientific, Oxford, Edinburgh,, 1968).

5. "Melanoma and Other Skin Cancers", in *What You Need To Know About* (National Institutes of Health, 2010).

6. N. A. Soter and H. P. Baden, *Pathophysiology of dermatologic diseases* (McGraw-Hill, New York, 1984).

7. R. Marks, G. Rennie, and T. S. Selwood, Lancet **1**, 8589, 795 (1988).

8. M. S. Arons and S. Hurwitz, Plastic and reconstructive surgery **72**, 3, 355 (1983).

9. L. Titus-Ernstoff, P. H. Duray, M. S. Ernstoff, R. L. Barnhill, P. L. Horn, and J. M. Kirkwood, Cancer Res **48**, 4, 1016 (1988).

10. J. Slade, A. A. Marghoob, T. G. Salopek, D. S. Rigel, A. W. Kopf, and R. S. Bart, J Am Acad Dermatol **32**, 3, 479 (1995).

11. C. S. Wong, R. C. Strange, and J. T. Lear, BMJ **327**, 7418, 794 (2003).

12. J. W. Patterson, M. R. Wick, and A. R. o. Pathology, *Nonmelanocytic tumors of the skin* (American Registry of Pathology, 2006).

13. C. M. Lawrence and N. H. Cox, *Physical signs in dermatology* (Mosby, 2002).

14. S. J. Salasche, J Am Acad Dermatol **42**, 1 Pt 2, 4 (2000).

15. J. P. Callen, D. R. Bickers, and R. L. Moy, J Am Acad Dermatol **36**, 4, 650 (1997).

16. D. S. Rigel, J. Russak, and R. Friedman, CA Cancer J Clin **60**, 5, 301 (2010).

17. M. Quinn and National Statistics (Great Britain), *Cancer atlas of the United Kingdom and Ireland 1991-2000* (Palgrave Macmillan, Basingstoke, Hampshire ;, 2005).

18. M. H. Brownstein, B. B. Kazam, and K. Hashimoto, Arch Dermatol **113**, 11, 1572 (1977).

19. A. J. Sober and J. M. Burstein, Cancer **75**, 2 Suppl, 645 (1995).

20. D. S. Rigel, J. K. Rivers, A. W. Kopf, R. J. Friedman, A. F. Vinokur, E. R. Heilman, and M. Levenstein, Cancer **63**, 2, 386 (1989).

21. I. Zalaudek, J. Kreusch, J. Giacomel, G. Ferrara, C. Catricala, and G. Argenziano, J Am Acad Dermatol **63**, 3, 377 (2010).

22. V. McGovern, Environ Health Perspect **111**, 14, A770 (2003).

23. D. S. Rigel and J. A. Carucci, CA Cancer J Clin **50**, 4, 215 (2000).

24. S. M. Dinehart, J Am Acad Dermatol **42**, 1 Pt 2, 25 (2000).

25. B. D. Wilson, T. S. Mang, H. Stoll, C. Jones, M. Cooper, and T. J. Dougherty, Arch Dermatol **128**, 12, 1597 (1992).

26. J. Larkin and M. Gore, Clin Evid (Online) **2008** (2008).

27. M. F. Mitchell, S. B. Cantor, N. Ramanujam, G. Tortolero-Luna, and R. Richards-Kortum, Obstetrics and gynecology **93**, 3, 462 (1999).

28. N. Ramanujam, Neoplasia **2**, 1-2, 89 (2000).

29. N. Ramanujam, M. F. Mitchell, A. Mahadevan, S. Thomsen, A. Malpica, T. Wright, N. Atkinson, and R. Richards-Kortum, Lasers Surg Med **19**, 1, 63 (1996).

30. L. Brancaleon, A. J. Durkin, J. H. Tu, G. Menaker, J. D. Fallon, and N. Kollias, Photochem Photobiol **73**, 2, 178 (2001).

31. R. Gillies, G. Zonios, R. R. Anderson, and N. Kollias, J Invest Dermatol **115**, 4, 704 (2000).

32. T. M. Breslin, F. Xu, G. M. Palmer, C. Zhu, K. W. Gilchrist, and N. Ramanujam, Ann Surg Oncol **11**, 1, 65 (2004).

33. P. K. Gupta, S. K. Majumder, and A. Uppal, Lasers Surg Med **21**, 5, 417 (1997).

34. G. M. Palmer, P. J. Keely, T. M. Breslin, and N. Ramanujam, Photochem Photobiol **78**, 5, 462 (2003).

35. W. C. Lin, S. A. Toms, M. Johnson, E. D. Jansen, and A. Mahadevan-Jansen, Photochem Photobiol **73**, 4, 396 (2001).

36. W. C. Lin, S. A. Toms, M. Motamedi, E. D. Jansen, and A. Mahadevan-Jansen, J Biomed Opt **5**, 2, 214 (2000).

37. N. Ramanujam, M. F. Mitchell, A. Mahadevan, S. Thomsen, A. Malpica, T. Wright, N. Atkinson, and R. Richards-Kortum, Lasers Surg Med **19**, 1, 46 (1996).

38. A. Mahadevan-Jansen, "Raman Spectroscopy: From Benchtop to Bedside", in *Biomedical Photonics Handbook*, T. Vo Dinh, Ed. (CRC Press, Boca Raton, FL, 2003), p. 30:1.

39. A. Mahadevan-Jansen and R. Richards-Kortum, J Biomed Opt **1**, 1, 31 (1996).

40. E. M. Kanter, E. Vargis, S. Majumder, M. D. Keller, E. Woeste, G. G. Rao, and A. Mahadevan-Jansen, J Biophotonics **2**, 1-2, 81 (2009).

41. A. Mahadevan-Jansen, M. F. Mitchell, N. Ramanujam, A. Malpica, S. Thomsen, U. Utzinger, and R. Richards-Kortum, Photochem Photobiol **68**, 1, 123 (1998).

42. P. R. Jess, D. D. Smith, M. Mazilu, K. Dholakia, A. C. Riches, and C. S. Herrington, Int J Cancer **121**, 12, 2723 (2007).

43. L. E. Kamemoto, A. K. Misra, S. K. Sharma, M. T. Goodman, H. Luk, A. C. Dykes, and T. Acosta, Appl Spectrosc **64**, 3, 255 (2010).

44. C. J. Frank, R. L. McCreery, and D. C. Redd, Anal Chem **67**, 5, 777 (1995).

45. A. S. Haka, K. E. Shafer-Peltier, M. Fitzmaurice, J. Crowe, R. R. Dasari, and M. S. Feld, Cancer Res **62**, 18, 5375 (2002).

46. N. Stone, C. Kendall, J. Smith, P. Crow, and H. Barr, Faraday Discuss **126**, 141 (2004).

47. P. Crow, A. Molckovsky, N. Stone, J. Uff, B. Wilson, and L. M. WongKeeSong, Urology **65**, 6, 1126 (2005).

48. Z. Huang, A. McWilliams, H. Lui, D. I. McLean, S. Lam, and H. Zeng, Int J Cancer **107**, 6, 1047 (2003).

49. X. Bi, A. Walsh, A. Mahadevan-Jansen, and A. Herline, Dis Colon Rectum **54**, 1, 48 (2011).

50. L. P. Choo-Smith, H. G. Edwards, H. P. Endtz, J. M. Kros, F. Heule, H. Barr, J. S. Robinson, Jr., H. A. Bruining, and G. J. Puppels, Biopolymers **67**, 1, 1 (2002).

51. E. B. Hanlon, R. Manoharan, T. W. Koo, K. E. Shafer, J. T. Motz, M. Fitzmaurice, J. R. Kramer, I. Itzkan, R. R. Dasari, and M. S. Feld, Physics in medicine and biology **45**, 2, R1 (2000).

52. J. Serup, B. E. Jemec, and G. L. Grove, *Handbook of non-invasive methods and the skin* (CRC/Taylor & Francis, 2006).

53. E. M. Kanter, S. Majumder, E. Vargis, A. Robichaux-Viehoever, G. J. Kanter, H. Shappell, H. W. Jones, 3rd, and A. Mahadevan-Jansen, Journal of Raman spectroscopy : JRS **40**, 2, 205 (2009).

54. A. Mahadevan-Jansen, W. F. Mitchell, N. Ramanujam, U. Utzinger, and R. Richards-Kortum, Photochemistry and Photobiology **68**, 3, 427 (1998).

55. A. Mahadevan-Jansen, E. Vargis, E. M. Kanter, S. K. Majumder, M. D. Keller, R. B. Beaven, and G. G. Rao, Analyst **136**, 14, 2981 (2011).

56. E. Vargis, T. Byrd, D. Khabele, and A. Mahadevan-Jansen, Gynecologic Oncology **116**, 3, S156 (2010).

57. M. S. Bergholt, W. Zheng, K. Lin, K. Y. Ho, M. Teh, K. G. Yeoh, J. B. So, and Z. Huang, J Biomed Opt **16**, 3, 037003 (2011).

58. A. Molckovsky, L. M. W. K. Song, M. G. Shim, N. E. Marcon, and B. C. Wilson, Gastrointestinal Endoscopy **57**, 3, 396 (2003).

59. M. G. Shim, L. M. Song, N. E. Marcon, and B. C. Wilson, Photochem Photobiol **72**, 1, 146 (2000).

60. A. S. Haka, Z. Volynskaya, J. A. Gardecki, J. Nazemi, J. Lyons, D. Hicks, M. Fitzmaurice, R. R. Dasari, J. P. Crowe, and M. S. Feld, Cancer Res **66**, 6, 3317 (2006).

61. P. J. Caspers, G. W. Lucassen, R. Wolthuis, H. A. Bruining, and G. J. Puppels, Biospectroscopy **4**, 5 Suppl, S31 (1998).

62. C. Edwards, Current problems in dermatology **26**, 20 (1998).

63. H. G. M. Edwards, A. C. Williams, and B. W. Barry, Journal of Molecular Structure **347**, 379 (1995).

64. M. Gniadecka, O. Faurskov Nielsen, D. H. Christensen, and H. C. Wulf, J Invest Dermatol **110**, 4, 393 (1998).

65. L. Knudsen, C. K. Johansson, P. A. Philipsen, M. Gniadecka, and H. C. Wulf, Journal of Raman Spectroscopy **33**, 7, 574 (2002).

66. A. Nijssen, T. C. B. Schut, F. Heule, P. J. Caspers, D. P. Hayes, M. H. A. Neumann, and G. J. Puppels, Journal of Investigative Dermatology **119**, 1, 64 (2002).

67. M. Osada, M. Gniadecka, and H. C. Wulf, Exp Dermatol **13**, 6, 391 (2004).

68. M. Gniadecka, H. C. Wulf, N. N. Mortensen, O. F. Nielsen, and D. H. Christensen, Journal of Raman Spectroscopy **28**, 2-3, 125 (1997).

69. M. Gniadecka, H. C. Wulf, O. F. Nielsen, D. H. Christensen, and J. Hercogova, Photochem Photobiol **66**, 4, 418 (1997).

70. M. E. Darvin, C. Sandhagen, W. Koecher, W. Sterry, J. Lademann, and M. C. Meinke, J Biophotonics (2012).

71. I. V. Ermakov, M. R. Ermakova, W. Gellermann, and J. Lademann, J Biomed Opt **9**, 2, 332 (2004).

72. I. V. Ermakov, M. R. Ermakova, R. W. McClane, and W. Gellermann, Opt Lett **26**, 15, 1179 (2001).

73. T. R. Hata, T. A. Scholz, I. V. Ermakov, R. W. McClane, F. Khachik, W. Gellermann, and L. K. Pershing, J Invest Dermatol **115**, 3, 441 (2000).

74. N. Kollias and G. N. Stamatas, J Investig Dermatol Symp Proc **7**, 1, 64 (2002).

75. Z. Huang, H. Lui, X. K. Chen, A. Alajlan, D. I. McLean, and H. Zeng, J Biomed Opt **9**, 6, 1198 (2004).

76. Z. Huang, H. Zeng, I. Hamzavi, D. I. McLean, and H. Lui, Opt Lett **26**, 22, 1782 (2001).

77. J. Wohlrab, A. Vollmann, S. Wartewig, W. C. Marsch, and R. Neubert, Biopolymers **62**, 3, 141 (2001).

78. J. Zhao, H. Lui, D. I. McLean, and H. Zeng, Conf Proc IEEE Eng Med Biol Soc **2008**, 3107 (2008).

79. J. Zhao, H. Lui, D. I. McLean, and H. Zeng, Skin Res Technol **14**, 4, 484 (2008).

80. M. Gniadecka, P. A. Philipsen, S. Sigurdsson, S. Wessel, O. F. Nielsen, D. H. Christensen, J. Hercogova, K. Rossen, H. K. Thomsen, R. Gniadecki, L. K. Hansen, and H. C. Wulf, J Invest Dermatol **122**, 2, 443 (2004).

81. Z. Huang, H. Lui, D. I. McLean, M. Korbelik, and H. Zeng, Photochem Photobiol **81**, 5, 1219 (2005).

82. S. Sigurdsson, P. A. Philipsen, L. K. Hansen, J. Larsen, M. Gniadecka, and H. C. Wulf, IEEE Trans Biomed Eng **51**, 10, 1784 (2004).

83. H. Lui, J. Zhao, D. McLean, and H. Zeng, Cancer Res **72**, 10, 2491 (2012).

84. H. C. Broding, A. van der Pol, J. de Sterke, C. Monse, M. Fartasch, and T. Bruning, Journal Der Deutschen Dermatologischen Gesellschaft **9**, 8, 618 (2011).

85. D. Huang, W. Zhang, H. Zhong, H. Xiong, X. Guo, and Z. Guo, J Biomed Opt **17**, 1, 015004 (2012).

86. P. J. Caspers, G. W. Lucassen, E. A. Carter, H. A. Bruining, and G. J. Puppels, J Invest Dermatol **116**, 3, 434 (2001).

87. P. J. Caspers, G. W. Lucassen, and G. J. Puppels, Biophys J **85**, 1, 572 (2003).

88. L. Chrit, P. Bastien, B. Biatry, J. T. Simonnet, A. Potter, A. M. Minondo, F. Flament, R. Bazin, G. D. Sockalingum, F. Leroy, M. Manfait, and C. Hadjur, Biopolymers **85**, 4, 359 (2007).

89. M. Forster, M. A. Bolzinger, M. R. Rovere, O. Damour, G. Montagnac, and S. Briancon, Skin Pharmacol Physiol **24**, 2, 103 (2011).

90. M. Pudlas, S. Koch, C. Bolwien, S. Thude, N. Jenne, T. Hirth, H. Walles, and K. Schenke-Layland, Tissue engineering. Part C, Methods **17**, 10, 1027 (2011).

91. G. N. Stamatas, J. Nikolovski, M. C. Mack, and N. Kollias, International journal of cosmetic science **33**, 1, 17 (2011).

92. J. Choi, J. Choo, H. Chung, D. G. Gweon, J. Park, H. J. Kim, S. Park, and C. H. Oh, Biopolymers **77**, 5, 264 (2005).

93. M. Forster, M. A. Bolzinger, G. Montagnac, and S. Briancon, European journal of dermatology : EJD **21**, 6, 851 (2011).

94. M. Larraona-Puy, A. Ghita, A. Zoladek, W. Perkins, S. Varma, I. H. Leach, A. A. Koloydenko, H. Williams, and I. Notingher, J Biomed Opt **14**, 5, 054031 (2009).

95. M. Larraona-Puy, A. Ghita, A. Zoladek, W. Perkins, S. Varma, I. H. Leach, A. A. Koloydenko, H. Williams, and I. Notingher, Journal of Molecular Structure **993**, 1-3, 57 (2011).

96. C. A. Patil, C. L. Arrasmith, M. A. Mackanos, D. L. Dickensheets, and A. Mahadevan-Jansen, Biomed Opt Express **3**, 3, 488 (2012).

97. C. A. Patil, N. Bosschaart, M. D. Keller, T. G. van Leeuwen, and A. Mahadevan-Jansen, Optics Letters **33**, 10, 1135 (2008).

98. C. A. Lieber, S. K. Majumder, D. L. Ellis, D. D. Billheimer, and A. Mahadevan-Jansen, Lasers Surg Med **40**, 7, 461 (2008).

99. C. A. Lieber, H. E. Nethercott, and M. H. Kabeer, Biomed Opt Express **1**, 3, 975 (2010).

100. C. A. Lieber and A. Mahadevan-Jansen, Applied Spectroscopy **57**, 11, 1363 (2003).

101. J. T. Motz, S. J. Gandhi, O. R. Scepanovic, A. S. Haka, J. R. Kramer, R. R. Dasari, and M. S. Feld, J Biomed Opt **10**, 3, 031113 (2005).

102. A. Alimova, R. Chakraverty, R. Muthukattil, S. Elder, A. Katz, V. Sriramoju, S. Lipper, and R. R. Alfano, Journal of photochemistry and photobiology. B, Biology **96**, 3, 178 (2009).

103. K. L. A. Chan, G. J. Zhang, M. Tomic-Canic, O. Stojadinovic, B. Lee, C. R. Flach, and R. Mendelsohn, Journal of Cellular and Molecular Medicine **12**, 5B, 2145 (2008).

104. N. J. Crane and E. A. Elster, J Biomed Opt **17**, 1, 010902 (2012).

105. L. Chrit, P. Bastien, G. D. Sockalingum, D. Batisse, F. Leroy, M. Manfait, and C. Hadjur, Skin Pharmacol Physiol **19**, 4, 207 (2006).

106. M. Egawa, T. Hirao, and M. Takahashi, Acta dermato-venereologica **87**, 1, 4 (2007).

107. E. E. Lawson, H. G. Edwards, B. W. Barry, and A. C. Williams, Journal of drug targeting **5**, 5, 343 (1998).

108. A. C. Williams, B. W. Barry, H. G. Edwards, and D. W. Farwell, Pharm Res **10**, 11, 1642 (1993).

109. A. Cerussi, S. Siavoshi, A. Durkin, C. Chen, W. Tanamai, D. Hsiang, and B. J. Tromberg, Appl Opt **48**, 21, 4270 (2009).

110. A. Nath, K. Rivoire, S. Chang, D. Cox, E. N. Atkinson, M. Follen, and R. Richards-Kortum, J Biomed Opt **9**, 3, 523 (2004).

111. R. Reif, M. S. Amorosino, K. W. Calabro, O. A'Amar, S. K. Singh, and I. J. Bigio, J Biomed Opt **13**, 1, 010502 (2008).

112. Y. Ti and W. C. Lin, Opt Express **16**, 6, 4250 (2008).

113. P. Colombo, A. Baldassarri, M. Del Corona, L. Mascaro, and S. Strocchi, Magnetic resonance imaging **22**, 1, 93 (2004).

114. L. Friedman, G. H. Glover, D. Krenz, and V. Magnotta, Neuroimage **32**, 4, 1656 (2006).

115. Y. Guo, P. W. Franks, T. Brookshire, and P. Antonio Tataranni, Obesity research **12**, 12, 1925 (2004).

116. B. M. Pikkula, O. Shuhatovich, R. L. Price, D. M. Serachitopol, M. Follen, N. McKinnon, C. MacAulay, R. Richards-Kortum, J. S. Lee, E. N. Atkinson, and D. D. Cox, J Biomed Opt **12**, 3, 034014 (2007).

117. R. M. Zucker and J. M. Lerner, Microsc Res Tech **68**, 5, 307 (2005).

118. J. D. Rodriguez, B. J. Westenberger, L. F. Buhse, and J. F. Kauffman, Analyst **136**, 20, 4232 (2011).

119. B. W. Barry, H. G. M. Edwards, and A. C. Williams, Journal of Raman Spectroscopy **23**, 11, 641 (1992).

120. A. Mahadevan-Jansen and R. Richards-Kortum, Journal of Biomedical Optics **1**, 1, 31 (1996).

121. R. S. Greene, D. T. Downing, P. E. Pochi, and J. S. Strauss, J Invest Dermatol **54**, 3, 240 (1970).

122. K. Robertson and J. L. Rees, Acta dermato-venereologica **90**, 4, 368 (2010).

123. J. Sandby-Moller, T. Poulsen, and H. C. Wulf, Acta dermato-venereologica **83**, 6, 410 (2003).

124. E. Vargis, T. Byrd, Q. Logan, D. Khabele, and A. Mahadevan-Jansen, J Biomed Opt **16**, 11, 117004 (2011).